Strong-coupling analysis of two-dimensional O(N) σ models with $N \geqslant 3$ on square, triangular, and honeycomb lattices

Massimo Campostrini, Andrea Pelissetto, Paolo Rossi, and Ettore Vicari

Dipartimento di Fisica dell'Università and INFN, I-56126 Pisa, Italy

Recently generated long strong-coupling series for the two-point Green's functions of asymptotically free O(N) lattice σ models are analyzed, focusing on the evaluation of dimensionless renormalization-group-invariant ratios of physical quantities and applying resummation techniques to series in the inverse temperature β and in the energy E. Square, triangular, and honeycomb lattices are considered, as a test of universality and in order to estimate systematic errors. Large-N solutions are carefully studied in order to establish benchmarks for series coefficients and resummations. Scaling and universality are verified. All invariant ratios related to the large-distance properties of the two-point functions vary monotonically with N, departing from their large-N values only by a few per mille even down to $N = 3$. [S0556-2821(96)00414-6]

I. INTRODUCTION

The properties of physical systems in the vicinity of a critical point, such as critical exponents and amplitude ratios, can be extracted by a variety of methods, ranging from exact solutions to Monte Carlo simulations.

In the absence of exact results, one of the most successful approaches is based on the investigation of the strong-coupling series expansion, which enjoys the property of a finite radius of convergence, often (but not necessarily) coinciding with the extent of the high-temperature phase. More generally, when no singular points occur on the real axis of the complex coupling plane, it is possible to exploit strong-coupling results even beyond the convergence radius by analytic continuations, which are based on appropriate resummation methods. Extending the length of the strong-coupling series and improving the accuracy of the resummations are, therefore, the two most compelling tasks within this approach to the study of the behavior of systems in the critical region.

As part of an extended program of strong-coupling calculations we have recently computed an extended series expansion of all nontrivial two-point Green's functions

$$G(x) = \langle \vec{s}(0) \cdot \vec{s}(x) \rangle \tag{1}$$

for the nearest-neighbor lattice formulation of two-dimensional O(N) σ models on the square, triangular, and honeycomb lattices, respectively up to 21st, 15th, and 30th order in the strong-coupling expansion parameter β. A complete presentation of our strong-coupling computations for O(N) σ models in two and three dimensions will appear in a forthcoming paper. A preliminary report of our calculations can be found in Ref. [1].

The relevance of a better understanding of two-dimensional (2D) O(N) σ models cannot be overestimated. They appear in condensed matter literature as prototype models for critical phenomena that are essentially restricted to two-dimensional layers, including some instances of high-T_c superconductivity. Moreover, they can be employed as model field theories sharing some of the most peculiar features of four-dimensional gauge theories, such as asymptotic freedom and spontaneous mass generation. This last statement must, however, be qualified, since the above-mentioned properties, according to common lore, are possessed only by those (2D) O(N) models such that $N > 2$.

We focus here on these asymptotically free models, analyzing their strong-coupling expansion in order to extract information that may be relevant to the description of their continuum limit ($\beta \to \infty$), assuming $\beta_c = \infty$ to be the only singularity on the real axis. This hypothesis is favored by all numerical evidence as well as by the successful application of the extrapolation techniques that we shall discuss in the present paper. The analysis of our strong-coupling series for models with $N \leqslant 2$ is presented in Ref. [2].

It is obviously quite hard to imagine that strong-coupling techniques may be really accurate in describing the divergent behavior of such quantities as the correlation length and the magnetic susceptibility. Nevertheless, as our calculations will explicitly confirm, the strong-coupling analysis may provide quite accurate continuum-limit estimates when applied directly to dimensionless, renormalization-group-invariant ratios of physical quantities. Two basic ideas will make this statement more convincing.

(i) For any dimensionless, renormalization-group-invariant ratio $R(\beta)$, when β is sufficiently large we may expect a behavior

$$R(\beta) - R^* \sim \frac{1}{\xi^2(\beta)}, \tag{2}$$

where R^* is the fixed point (continuum) value and ξ is the (diverging) correlation length. Hence a reasonable estimate of R^* may be obtained at the values of β corresponding to large but finite correlation lengths, where the function $R(\beta)$ flattens. This is essentially the same idea underlying Monte Carlo studies of asymptotically free theories, based on the identification of the so-called scaling region.

(ii) On physical grounds, it is understandable that β is not necessarily the most convenient variable to parametrize phe-

nomena occurring around $\beta = \infty$. An interesting alternative is based on the observation that the strong-coupling series of the internal energy,

$$E = \beta + O(\beta^3), \qquad (3)$$

may be inverted to give β as a series in E. This series may be substituted into other strong-coupling expansions, obtaining expressions for physical quantities as power series in E. It might now be easier to reach the continuum limit, since it now occurs at a finite value of the expansion variable, i.e., $E \to 1$.

We hope to convince the reader that, by exploiting these ideas, state-of-the-art strong-coupling calculations can be made at least as accurate as the best Monte Carlo simulations presently available, when applied to dimensionless renormalization-group-invariant quantities.

We must stress that the analysis of the strong-coupling series calculated on different lattices offers a possibility of testing universality, and, on the other hand, once universality is assumed, it represents a further check for possible systematic errors and allows their quantitative estimate; this estimate is usually a difficult task in strong-coupling extrapolation methods such as those based on Padé approximants and their generalizations.

Our physical intuition of the behavior of O(N) models is strongly guided by our knowledge of their large-N behavior, and by the evidence of a very weak dependence on N of the dimensionless ratios. In order to extend our understanding to those lattices that have not till now received a systematic treatment, and also in order to establish a benchmark for the strong-coupling analysis, we decided to start our presentation with a detailed comparative study of the large-N limit of various lattices, in the nearest-neighbor formulation. To the best of our knowledge, only the large-N solution on the square lattice was already known explicitly [3].

The paper is organized as follows.

In Sec. II we present the large-N limit solution of O(N) σ models on the square, triangular, and honeycomb lattices, in the nearest-neighbor formulation, calculating several physical quantities and showing explicitly the expected universality properties. The triangular- and honeycomb-lattice results are original, and possess some intrinsic reasons of interest. However, readers willing to focus on square-lattice results are advised to jump to Sec. III after reading Secs. II A and II B, where the notation is fixed.

Section III is devoted to a detailed analysis of the available strong-coupling series of $G(x)$ and other physical quantities on the square, triangular, and honeycomb lattices. Most of the results we shall show there concern the $N = 3$ model. The basic motivation for this choice lies in the observation that all dependence on N is monotonic between 3 and ∞; hence the discussion of higher-N results would be only a boring repetition of the considerations presented here. The reader not interested in the analysis of triangular and honeycomb lattices may skip most of the discussion, by focusing on Sec. III B, where further definitions are introduced and the square-lattice series are analyzed, and on Sec. III E, where all conclusions are drawn.

Appendixes A and B provide the derivation and the technical details of the large-N calculations on the triangular and honeycomb lattices, respectively. We present as well the calculation of the Λ parameters. Appendix C is a study of the complex-temperature singularities of the $N = \infty$ partition functions on the triangular and honeycomb lattices. In Appendixes D, E, and F we present, for selected values of N, the strong-coupling series of some relevant quantities on the square, triangular, and honeycomb lattices, respectively.

II. THE LARGE-N LIMIT OF LATTICE O(N) σ MODELS

A. The large-N saddle point equation

The nearest-neighbor lattice formulations on square, triangular, and honeycomb lattices are defined by the action

$$S_L = -N\beta \sum_{\text{links}} \vec{s}_{x_l} \cdot \vec{s}_{x_r}, \quad \vec{s}_x \cdot \vec{s}_x = 1, \qquad (4)$$

where $\vec{s}$ is an N-component vector, the sum is performed over all links of the lattice, and x_l, x_r indicate the sites at the ends of each link. The coordination number is $c = 4, 6, 3$, respectively, for the square, triangular, and honeycomb lattice. The lattice spacing a, which represents the length unit, is defined to be the length of a link. The volume per site is then $v_s = 1, \sqrt{3}/2$, and $3\sqrt{3}/4$ (in unit of a^2), respectively, for the square, triangular, and honeycomb lattice.

Straightforward calculations show that the correct continuum limit of O(N) σ models,

$$S = \frac{N}{2t} \int d^2x \, \partial_\mu \vec{s}(x) \cdot \partial_\mu \vec{s}(x), \quad \vec{s}(x) \cdot \vec{s}(x) = 1, \qquad (5)$$

is obtained by identifying

$$t = \frac{1}{\beta}, \frac{1}{\sqrt{3}\beta}, \frac{\sqrt{3}}{\beta}, \qquad (6)$$

respectively, for the square, triangular, and honeycomb lattice. Notice that

$$\lambda \equiv t\beta = \frac{4v_s}{c} \qquad (7)$$

is the distance between nearest-neighbor sites of the dual lattice in units of the lattice spacing a.

When the number of field components N per site goes to infinity, one can use a saddle point equation to evaluate the partition function. Replacing the constraint $\vec{s}_x^2 = 1$ by a Fourier integral over a conjugate variable α_x, we write the partition function as

$$Z \propto \int \prod_x d\vec{s}_x \, \delta(\vec{s}_x^2 - 1) \exp\left(N\beta \sum_{\text{links}} \vec{s}_{x_l} \cdot \vec{s}_{x_r} \right)$$

$$\propto \int \prod_x d\phi_x d\alpha_x \exp\left[N\left(\sum_x i \frac{\alpha_x}{2}(1 - \phi_x^2) \right.\right.$$

$$\left.\left. - \frac{\beta}{2} \sum_{\text{links}} (\phi_{x_l} - \phi_{x_r})^2 \right) \right]. \qquad (8)$$

Integrating out the ϕ variables we arrive at the expression

$$Z \propto \int d\alpha_x \exp\left[\frac{N}{2}\left(\sum_x i\alpha_x - \mathrm{Tr}\ln R\right)\right], \quad (9)$$

where

$$R_{xy} = -\frac{1}{t}\Delta_{xy} + i\alpha_x\delta_{xy}, \quad (10)$$

and Δ_{xy} is a generalized Laplacian operator, such that

$$\lambda\sum_{\text{links}}(\phi_{x_l} - \phi_{x_r})^2 = -\sum_{x,y}\phi_x\Delta_{xy}\phi_y. \quad (11)$$

The large-N limit solution is obtained from the variational equation with respect to α_x. Looking for a translation-invariant solution we set

$$i\alpha_x = \frac{v_s}{t}z. \quad (12)$$

The matrix R then becomes

$$R_{xy} = \frac{1}{t}[-\Delta_{xy} + zv_s\delta_{xy}], \quad (13)$$

and the saddle point equation is written as

$$1 = \lim_{N_s\to\infty}\frac{1}{N_s}\mathrm{Tr}R^{-1}, \quad (14)$$

where N_s is the number of sites.

The large-N fundamental two-point Green's function is obtained by

$$G(x-y) = R_{xy}^{-1}. \quad (15)$$

In order to calculate the trace of R^{-1}, the easiest procedure consists in Fourier transforming the operator R. Such a transformation is straightforward on lattices, such as square and triangular lattices, whose sites are related by a translation group, and in these cases it yields the diagonalization of the matrix R_{xy}. The honeycomb lattice, not possessing a full translation symmetry, presents some complications. In this case a partial diagonalization of R_{xy} can be achieved following the procedure outlined in Ref. [4].

B. The square lattice

Turning to the momentum space, the variational equation becomes

$$\frac{1}{t} = \beta = \int_{-\pi}^{\pi}\frac{d^2k}{(2\pi)^2}\frac{1}{\hat{k}^2 + z} = \frac{1}{2\pi}\rho_s(z)K(\rho_s(z)), \quad (16)$$

where

$$\rho_s(z) = \left(1 + \frac{1}{4}z\right)^{-1}, \quad (17)$$

and K is the complete integral of the first kind.

Let us define the moments of $G(x)$,

$$m_{2j} \equiv \sum_x (x^2)^j G(x). \quad (18)$$

Straightforward calculations lead to the results

$$\chi \equiv m_0 = \frac{t}{z}, \quad (19)$$

$$\xi_G^2 \equiv M_G^{-2} \equiv \frac{m_2}{4\chi} = \frac{1}{z}, \quad (20)$$

$$u \equiv \frac{m_2^2}{\chi m_4} = \frac{1}{4}\left(1 + \frac{z}{16}\right)^{-1}. \quad (21)$$

Notice that in the large-N limit the renormalization constant of the fundamental field is $Z = t$. u is a renormalization-group-invariant quantity.

The mass gap should be extracted from the long-distance behavior of the two-point Green's function, which is also related to the imaginary momentum singularity of the Fourier transform of $G(x)$. In the absence of a strict rotation invariance, one actually may define different estimators of the mass gap having the same continuum limit. On the square lattice one may consider μ_s and μ_d obtained, respectively, by the equations

$$\tilde{G}^{-1}(p_1 = i\mu_s, p_2 = 0) = 0,$$

$$\tilde{G}^{-1}\left(p_1 = i\frac{\mu_d}{\sqrt{2}}, p_2 = i\frac{\mu_d}{\sqrt{2}}\right) = 0. \quad (22)$$

μ_s and μ_d determine, respectively, the long-distance behavior of the side and diagonal wall-wall correlations constructed with $G(x)$. In generalized Gaussian models, such as the large-N limit of O(N) models, it turns out convenient to define the quantities

$$M_s^2 = 2(\cosh\mu_s - 1),$$

$$M_d^2 = 4\left(\cosh\frac{\mu_d}{\sqrt{2}} - 1\right). \quad (23)$$

In the continuum limit

$$\frac{M_s}{\mu_s}, \frac{M_d}{\mu_d} \to 1; \quad (24)$$

therefore M_s and M_d may also be used as estimators of the mass gap.

In the large-N limit,

$$M_s^2 = M_d^2 = z = M_G^2. \quad (25)$$

The rotational invariance of $G(x)$ at large distance, $d \gg \xi$, is checked by the ratios μ_s/μ_d. Using the above results one can evaluate the scaling violation terms:

$$\frac{\mu_s}{\mu_d} = \frac{\ln(\frac{1}{2}\sqrt{z} + \sqrt{1 + \frac{1}{4}z})}{\sqrt{2}\ln[(1/2\sqrt{2})\sqrt{z} + \sqrt{1 + \frac{1}{8}z}]}$$

$$= 1 - \frac{1}{48}z + \frac{71}{23\,040}z^2 + O(z^3). \qquad (26)$$

Another test of scaling is provided by the ratio

$$\frac{\mu_s}{M_G} = \frac{2}{\sqrt{z}}\ln\left(\frac{\sqrt{z}}{2} + \sqrt{1 + \frac{z}{4}}\right) = 1 - \frac{1}{24}z + \frac{3}{640}z^2 + O(z^3).$$
$$(27)$$

The internal energy can be easily calculated, obtaining

$$E \equiv \langle \vec{s}_x \cdot \vec{s}_{x+\mu} \rangle = R_{x,x+\mu}^{-1} = 1 - \frac{1}{4\beta} + \frac{z}{4}. \qquad (28)$$

Therefore

$$\frac{1}{2}\sum_\mu \langle (\vec{s}_{x+\mu} - \vec{s}_x)^2 \rangle = \frac{1}{2\beta} - \frac{z}{2}, \qquad (29)$$

where the term proportional to z is related to the condensate T of the trace of the energy-momentum tensor [5]

$$\frac{\beta(t)}{2t^2}\partial_\mu \vec{s}(x) \cdot \partial_\mu \vec{s}(x). \qquad (30)$$

In the large-N limit,

$$\beta(t) = -\frac{1}{2\pi}t^2; \qquad (31)$$

therefore, from expression (28) we deduce

$$\frac{T}{M_G^2} = \frac{1}{4\pi}. \qquad (32)$$

Another interesting quantity which can be evaluated in the large-N limit is the zero-momentum four-point renormalized coupling constant, defined by

$$g_r = -\frac{\chi_4}{\chi^2 \xi_G^2} \qquad (33)$$

where

$$\chi_4 = \sum_{x,y,z} \langle \vec{s}_0 \cdot \vec{s}_x \vec{s}_y \cdot \vec{s}_z \rangle_c. \qquad (34)$$

g_r is zero in the large-N limit, where the theory is Gaussian-like and thus $\chi_4 = 0$. Its value in the continuum limit,

$$g_r^* = \frac{8\pi}{N} + O\left(\frac{1}{N^2}\right), \qquad (35)$$

can also be evaluated in the large-N expansion of the continuum formulation of the O(N) models [6]. On the square lattice, by using the saddle point equation we find

$$Ng_r = -2\frac{\partial \ln z}{\partial \beta}, \qquad (36)$$

which can be made more explicit by writing

$$Ng_r = 4\pi\frac{1+\rho_s}{\rho_s E(\rho_s)} = 8\pi\left[1 + \frac{z}{8}\left(\ln\frac{z}{32} + 2\right) + O(z^2)\right],$$
$$(37)$$

where E is an elliptic function.

All the above results can be expressed as functions of β by solving the saddle point equation. Concerning asymptotic scaling, and therefore solving the saddle point equation at large β, one finds

$$M_G \simeq 4\sqrt{2}\exp\left(-\frac{2\pi}{t}\right). \qquad (38)$$

The analytic structure of the various observables has been investigated in Ref. [7]. The complex-β singularities are square-root branch points; indeed quantities such as χ and ξ_G^2 behave as

$$A(\beta) + B(\beta)\sqrt{\beta - \beta_s} \qquad (39)$$

around a singular point β_s, where $A(\beta)$ and $B(\beta)$ are regular in the neighborhood of β_s. The singularities closest to the origin are located at $\bar{\beta} = 0.321\,62(\pm 1 \pm i)$. Such singularities determine the convergence radius of the strong-coupling expansion, which is therefore $\beta_r = 0.454\,84$, corresponding to a correlation length $\xi_G = 3.171\,60$.

C. The triangular lattice

On the triangular lattice, using the results of Appendix A, the saddle point equation can be written as

$$\frac{1}{t} = \sqrt{3}\beta = \int_{-\pi}^{\pi}\frac{dk_1}{2\pi}\int_{-2\pi/\sqrt{3}}^{2\pi/\sqrt{3}}\frac{dk_2}{2\pi}\frac{1}{\Delta(k) + z} \qquad (40)$$

where

$$\Delta(k) = 4\left[1 - \frac{1}{3}\left(\cos k_1 + 2\cos\frac{k_1}{2}\cos\frac{\sqrt{3}k_2}{2}\right)\right] \qquad (41)$$

and the momentum integration is performed over the Brillouin zone corresponding to a triangular lattice. By rather straightforward calculations (making use also of some of the formulas of Ref. [8]) the saddle point equation can be written as

$$\frac{1}{t} = \sqrt{3}\beta = \frac{1}{2\pi}\left(1 + \frac{z}{6}\right)^{-1/4}\rho_t(z)K(\rho_t(z)), \qquad (42)$$

where

$$\rho_t(z) = \left(1 + \frac{z}{6}\right)^{1/4}\left[\frac{1}{2} + \frac{z}{8} + \frac{1}{2}\left(1 + \frac{z}{6}\right)^{1/2}\right]^{-1/2}$$

$$\times\left[\frac{5}{2} + \frac{3z}{8} - \frac{3}{2}\left(1 + \frac{z}{6}\right)^{1/2}\right]^{-1/2}. \qquad (43)$$

Using the results of Appendix A one can find

$$\chi = \frac{t}{v_s z} = \frac{2}{3\beta z}, \tag{44}$$

$$\xi_G^2 \equiv M_G^{-2} = \frac{1}{z}, \tag{45}$$

$$u \equiv \frac{m_2^2}{\chi m_4} = \frac{1}{4}\left(1 + \frac{z}{16}\right)^{-1}. \tag{46}$$

An estimator of the mass gap μ_t can be extracted from the long-distance behavior of the wall-wall correlation function defined in Eq. (A7); indeed, for $x \gg 1$,

$$G_t^{(w)}(x) \propto e^{-\mu_t x}. \tag{47}$$

In the large-N limit one finds

$$M_t^2 \equiv \frac{8}{3}\left(\cosh\frac{\sqrt{3}}{2}\mu_t - 1\right) = z = M_G^2. \tag{48}$$

A test of scaling is provided by the ratio

$$\frac{\mu_t}{M_G} = \frac{2}{\sqrt{3z}}\text{arccosh}\left[1 + \frac{3}{8}z\right] = 1 - \frac{1}{32}z + \frac{9}{10\,240}z^2 + O(z^3), \tag{49}$$

where scaling violations are of the same order as those found on the square lattice for the corresponding quantity; cf. Eq. (27).

The internal energy is given by the expression

$$E = \langle \vec{s}_{x_l} \cdot \vec{s}_{x_r}\rangle = 1 - \frac{1}{6\beta} + \frac{z}{4}, \tag{50}$$

leading again to the result (32) for the condensate of the trace of the energy-momentum tensor, in agreement with universality.

We calculated g_r on the triangular lattice, finding the expression [in the derivation we made use of the saddle point equation (40)]

$$Ng_r = -\frac{2}{\sqrt{3}}\frac{\partial \ln z}{\partial \beta}, \tag{51}$$

which can be written in a more explicit form using Eq. (42):

$$Ng_r = 4\pi\left(1 + \frac{1}{6}z\right)^{1/4}\frac{1}{z}\left[\frac{E(\rho_t)}{1 - \rho_t^2}\frac{\partial \rho_t}{\partial z}\right.$$
$$\left. - \frac{1}{24}\left(1 + \frac{1}{6}z\right)^{-1}\rho_t K(\rho_t)\right]^{-1}$$
$$= 8\pi\left[1 + \frac{z}{8}\left(\ln\frac{z}{48} + \frac{11}{6}\right) + O(z^2)\right], \tag{52}$$

where the continuum value of Ng_r, obtained for $z \to 0$, is in agreement with the results (35) and (37).

In the weak-coupling region $t \to 0$ the saddle point equation leads to the asymptotic scaling formula

$$M_G \simeq 4\sqrt{3}\exp\left(-\frac{2\pi}{t}\right). \tag{53}$$

Equations (38) and (53) are in agreement with the large-N limit of the ratio of the Λ parameters of the square and triangular lattice formulations calculated in Appendix A [cf. Eq. (A13)] using perturbation theory.

We have investigated the analytic structure in the complex β plane. Details of such study are presented in Appendix C. As on the square lattice, the singularities are square-root branch points. Those closest to the origin are placed at $\bar{\beta} = 0.206\,711 \pm i\,0.181\,627$, leading to a convergence radius for the strong-coupling expansion $\beta_r = 0.275\,169$, which corresponds to a correlation length $\xi_G = 2.989\,25$.

D. The honeycomb lattice

The analysis of models defined on the honeycomb lattice presents a few subtleties caused by the fact that, unlike square and triangular lattices, not all sites are related by a translation, not allowing a straightforward definition of a Fourier transform. Nevertheless, observing that sites at even distance in the number of lattice links form triangular lattices, one can define a Fourier-like transformation that partially diagonalizes the Gaussian propagator (up to 2×2 matrices) [4]. In this section we present the relevant results; some details of their derivation are reported in Appendix B.

Using the expression of R^{-1} of Eq. (B4) we write the saddle point equation in the form

$$\frac{1}{t} = \frac{\beta}{\sqrt{3}} = \int_{-2\pi/3}^{2\pi/3}\frac{dk_1}{2\pi}\int_{-\pi/\sqrt{3}}^{\pi/\sqrt{3}}\frac{dk_2}{2\pi}\frac{1 + \frac{1}{4}z}{\Delta(k) + z(1 + \frac{1}{8}z)} \tag{54}$$

where

$$\Delta(k) = \frac{8}{9}\left[2 - \cos\frac{\sqrt{3}}{2}k_2\left(\cos\frac{3}{2}k_1 + \cos\frac{\sqrt{3}}{2}k_2\right)\right], \tag{55}$$

and integrating over the momentum we arrive at

$$\frac{1}{t} = \frac{\beta}{\sqrt{3}} = \frac{1}{2\pi}\left(1 + \frac{z}{4}\right)^{1/2}\rho_h(z)K(\rho_h(z)), \tag{56}$$

where

$$\rho_h(z) = \left(1 + \frac{z}{4}\right)^{1/2}\left(1 + \frac{3z}{8}\right)^{-3/2}\left(1 + \frac{z}{8}\right)^{-1/2}. \tag{57}$$

From Eq. (B4) we also derive

$$\chi = \frac{t}{v_s z} = \frac{4}{3\beta z}, \tag{58}$$

$$\xi_G^2 \equiv M_G^{-2} = \frac{1}{z}, \tag{59}$$

$$u = \frac{1}{4}\left(1 + \frac{z}{16}\right)^{-1}. \tag{60}$$

The two orthogonal wall-wall correlation functions $G_v^{(w)}(x)$ and $G_h^{(w)}(x)$ defined in Eqs. (B6) and (B7) allow one to define two estimators of the mass gap from their long-distance behavior:

$$G_v^{(w)}(x) \propto e^{-\mu_v x},$$

$$G_h^{(w)}(x) \propto e^{-\mu_h x}, \tag{61}$$

where x is the distance between the two walls in units of the lattice spacing. In the continuum limit $\mu_v = \mu_h$ and they both reproduce the physical mass propagating in the fundamental channel. As on the square and triangular lattices, it is convenient to define the quantities

$$M_v^2 = \frac{8}{9}\left(\cosh\frac{3\mu_v}{2} - 1\right),$$

$$M_h^2 = \frac{8}{3}\left(\cosh\frac{\sqrt{3}\mu_h}{2} - 1\right), \tag{62}$$

which, in the continuum limit, are also estimators of the mass gap. In the large-N limit one finds

$$M_v^2 = z\left(1 + \frac{z}{8}\right),$$

$$M_h^2 = z. \tag{63}$$

Notice that in the continuum large-N limit the result

$$\frac{M}{M_G} = 1, \tag{64}$$

where M is any mass-gap estimator, is found for all lattice formulations considered.

On the honeycomb lattice the maximal violation of full rotational symmetry occurs for directions differing by a $\pi/6$ angle, and therefore, taking into account its discrete rotational symmetry, also by a $\pi/2$ angle. So a good test of rotation invariance of $G(x)$ at large distance is provided by the ratio μ_v/μ_h:

$$\frac{\mu_v}{\mu_h} = \frac{\text{arccosh}[1 + \frac{9}{8}z(1 + \frac{1}{8}z)]}{\sqrt{3}\,\text{arccosh}[1 + \frac{3}{8}z]} = 1 + \frac{1}{640}z^2 + O(z^3). \tag{65}$$

As expected from the better rotational symmetry of the honeycomb lattice, rotation invariance is set earlier than for the square lattice; indeed, the $O(z)$ scaling violation is absent.

A test of scaling is provided by the ratio

$$\frac{\mu_h}{M_G} = \frac{2}{\sqrt{3z}}\text{arccosh}\left[1 + \frac{3}{8}z\right] = 1 - \frac{1}{32}z + \frac{9}{10\,240}z^2 + O(z^3), \tag{66}$$

where scaling violations are of the same order as those found on the square lattice for the corresponding quantity; cf. Eq. (27).
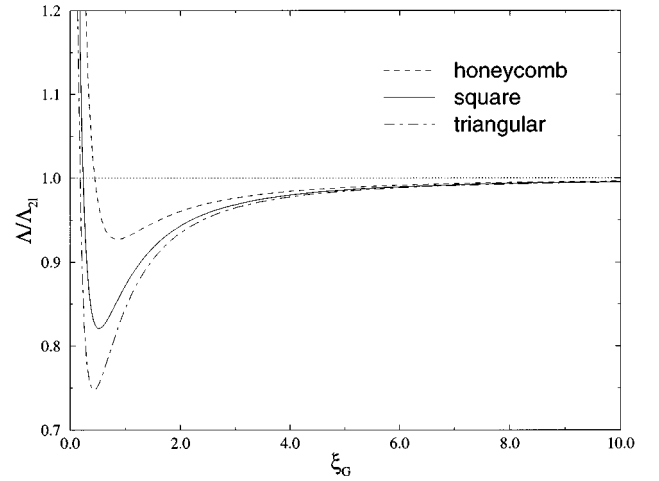
The internal energy is given by

FIG. 1. The large-N limit of the ratio between M_G and the corresponding weak-coupling asymptotic formulas for the square, triangular, and honeycomb lattices.

$$E = 1 - \frac{1}{3\beta} + \frac{z}{4} = 1 - \frac{1}{3\beta} + \frac{M_G^2}{4}, \tag{67}$$

where the term proportional to M_G^2 again verifies universality.

In the weak-coupling region $t \to 0$ the saddle point equation leads to the asymptotic scaling formula

$$M_G \simeq 4\exp\left(-\frac{2\pi}{t}\right). \tag{68}$$

Equations (38) and (68) are in agreement with the large-N limit of the ratio of the Λ parameters of the square and triangular lattice formulations calculated in Appendix B [cf. Eq. (B12)], using perturbation theory.

In Fig. 1 we compare asymptotic scaling from the various lattices considered, plotting the ratio between M_G and the corresponding asymptotic formula [cf. Eqs. (38), (53), and (68)]. Notice that in the large-N limit corrections to asymptotic scaling are $O(M_G^2)$, in that corrections $O(1/\ln M_G)$ are suppressed by a factor $1/N$.

We have investigated the analytic structure in the complex-temperature plane of the $N = \infty$ model on the honeycomb lattice (details are reported in Appendix C). As on the square and triangular lattices, singularities are square-root branch points, and those closest to the origin are placed on the imaginary axis at $\bar{\beta} = \pm i0.362\,095$. The convergence radius for the strong-coupling expansion is associated with a quite small correlation length: $\xi_G = 1.000\,02$.

III. CONTINUUM RESULTS FROM STRONG COUPLING

A. Analysis of the series

In this section we analyze the strong-coupling series of some of the physical quantities which can be extracted from the two-point fundamental Green's function. We especially consider dimensionless renormalization-group-invariant ratios, whose value in the scaling region, i.e., their asymptotic value for $\beta \to \infty$, concerns the continuum physics. Some

strong-coupling series for selected values of N are reported in Appendixes D, E, and F, respectively, for the square, triangular, and honeycomb lattices. The series in the energy are obtained by inverting the strong-coupling series of the energy $E = \beta + O(\beta^3)$ and substituting into the original series in β.

Our analysis of the series of dimensionless renormalization-group-invariant ratios of physical quantities, such as those defined in the previous section, is based on Padé approximant (PA) techniques. For a review on the resummation techniques, see Ref. [9].

PA's are expected to converge well to meromorphic analytic functions. More flexibility is achieved by applying the PA analysis to the logarithmic derivative (Dln-PA analysis), and therefore enlarging the class of functions which can be reproduced to those having branch-point singularities. The accuracy and the convergence of the PA's depend on how well the function considered, or its logarithmic derivative, can be reproduced by a meromorphic analytic function, and may change when considering different representations of the same quantity. By comparing the results from different series representations of the same quantity one may check for possible systematic errors in the resummation procedure employed.

In our analysis we constructed $[l/m]$ PA's and Dln-PA's of both the series in β and in the energy. l and m are the orders of the polynomials, respectively, at the numerator and at the denominator of the ratio forming the $[l/m]$ PA of the series at hand, or of its logarithmic derivative (Dln-PA). While $[l/m]$ PA's directly provide the quantity at hand, in a Dln-PA analysis one gets an $[l/m]$ approximant by reconstructing the original quantity from the $[l/m]$ PA of its logarithmic derivative, i.e., a $[l/m]$ Dln-PA of the series $A(x) = \sum_{i=0}^{\infty} a_i x^i$ is obtained from

$$A_{l/m}(x) = a_0 \exp\left(\int_0^x dx' \mathrm{Dln}_{l/m} A(x') \right), \qquad (69)$$

where $\mathrm{Dln}_{l/m} A(x)$ indicates the $[l/m]$ PA of the logarithmic derivative of $A(x)$.

We recall that an $[l/m]$ PA uses $n = l + m$ terms of the series, while an $[l/m]$ Dln-PA requires $n = l + m + 1$ terms. Continuum estimates are then obtained by evaluating the approximants of the energy series at $E = 1$, and those of the β series at a value of β corresponding to a reasonably large correlation length.

As final estimates we take the average of the results from the quasidiagonal (i.e., with $l \simeq m$) PA's using all available terms of the series. The errors we will display are just indicative, and give an idea of the spread of the results coming from different PA's. They are the square root of the variance around the estimate of the results, using also quasidiagonal PA's constructed from shorter series. Such errors do not always provide a reliable estimate of the uncertainty, which may be underestimated especially when the structure of the function (or of its logarithmic derivative) is not well approximated by a meromorphic analytic function. In such cases a more reliable estimate of the real uncertainty should come from the comparison of results from the analysis of different series representing the same quantity, which in general are not expected to have the same analytic structure.

In the remainder of this section we present the main results obtained from our strong-coupling analysis. Most of them will concern the $N = 3$ case.

B. The square lattice

On the square lattice we have calculated the two-point Green's function up to $O(\beta^{21})$, from which we have extracted strong-coupling series of the quantities E, χ, ξ_G^2, u, M_s^2, and M_d^2, already introduced in Sec. II B, and of the ratios $r \equiv M_s^2/M_d^2$ and $s \equiv M_s^2/M_G^2$. Some of the above series for selected values of N are reported in Appendix D. Our strong-coupling series represent a considerable extension of the 14th order calculations of Ref. [10], performed by means of a linked cluster expansion, which have been reelaborated and analyzed in Ref. [11]. We also mention recent works where the linked cluster expansion technique has been further developed and calculations of series up to 18th order [12] and 19th order [13] for $d = 2,3,4$ have been announced.

TABLE I. Summary of the large-N calculations in O(N) σ models on the square, triangular, and honeycomb lattices. All quantities appearing in this table have been defined in Sec. II.

	Square	Triangular	Honeycomb
c	4	6	3
v_s	1	$\sqrt{3}/2$	$3\sqrt{3}/4$
t	$4v_s/c\beta$	$4v_s/c\beta$	$4v_s/c\beta$
χ	$4/c\beta z$	$4/c\beta z$	$4/c\beta z$
M_G^2	z	z	z
u	$\frac{1}{4}\left(1 + \frac{1}{16}z\right)^{-1}$	$\frac{1}{4}\left(1 + \frac{1}{16}z\right)^{-1}$	$\frac{1}{4}\left(1 + \frac{1}{16}z\right)^{-1}$
E	$1 - 1/(c\beta) + \frac{1}{4}z$	$1 - 1/(c\beta) + \frac{1}{4}z$	$1 - 1/(c\beta) + \frac{1}{4}z$
M^2	$M_s^2 \equiv 2[\cosh\mu_s - 1] = z$	$M_t^2 \equiv \frac{8}{3}(\cosh(\sqrt{3}\mu_t/2) - 1) = z$	$M_h^2 \equiv \frac{8}{3}[\cosh(\sqrt{3}\mu_h/2) - 1] = z$
	$M_d^2 \equiv 4[\cosh(\mu_d/\sqrt{2}) - 1] = z$		$M_v^2 \equiv \frac{8}{9}\left[\cosh\left(\frac{3}{2}\mu_v\right) - 1\right] = z\left(1 + \frac{1}{8}z\right)$
$\Lambda_{\overline{\mathrm{MS}}}/\Lambda_L$	$4\sqrt{2}$	$4\sqrt{3}$	4

TABLE II. For various values of N we report the singularity closest to the origin on the square, triangular, and honeycomb lattices, as obtained by a Dln-PA analysis of the strong-coupling series of χ ($\overline{\beta}_\chi$) and ξ_G^2 ($\overline{\beta}_\xi$), and the corresponding convergence radius of the strong-coupling expansion β_r. The errors we display are related to the spread of the results coming from different quasidiagonal $[l/m]$ Dln-PA's using all available terms of the series, or a few less, while the difference between $\overline{\beta}_\chi$ and $\overline{\beta}_\xi$ should give an idea of the systematic error in the procedure.

Lattice	N	$\overline{\beta}_\chi$	$\overline{\beta}_\xi$	β_r
Square	3	$0.590(1)\pm i\, 0.156(1)$	$0.586(1)\pm i\, 0.157(1)$	0.61
	4	$0.557(10)\pm i\, 0.226(4)$	$0.555(5)\pm i\, 0.225(5)$	0.60
	8	$0.467(4)\pm i\, 0.298(3)$	$0.467(3)\pm i\, 0.293(1)$	0.55
	∞	$0.321621\ldots(1\pm i)$	$0.321621\ldots(1\pm i)$	$0.454841\ldots$
Triangular	3	$0.3582(2)\pm i\, 0.085(1)$	$0.357(1)\pm i\, 0.089(4)$	0.37
	4	$0.343(1)\pm i\, 0.121(1)$	$0.341(2)\pm i\, 0.124(2)$	0.36
	8	$0.2901(1)\pm i\, 0.1654(1)$	$0.283(4)\pm i\, 0.163(4)$	0.33
	∞	$0.206711\ldots\pm i\, 0.181627\ldots$	$0.206711\ldots\pm i\, 0.181627\ldots$	$0.275169\ldots$
Honeycomb	3	$\pm i\, 0.459(1)$	$\pm i\, 0.461(1)$	0.46
	4	$\pm i\, 0.4444(1)$	$\pm i\, 0.445(2)$	0.44
	8	$\pm i\, 0.4161(1)$	$\pm i\, 0.4169(2)$	0.42
	∞	$\pm i\, 0.362095\ldots$	$\pm i\, 0.362095\ldots$	$0.362095\ldots$

In order to investigate the analytic structure in the complex-β plane we have performed a study of the singularities of the Dln-PA's of the strong-coupling series of χ and ξ_G^2. As expected by asymptotic freedom, no indication of the presence of a critical point at a finite real value of β emerges from the strong-coupling analysis of $N \geq 3$ models, confirming earlier strong-coupling studies [11]. The singularities closest to the origin emerging from the Dln-PA analysis of χ and ξ_G^2 are located at a pair of complex conjugate points, rather close to the real axis in the $N=3$ case (where $\overline{\beta} \simeq 0.59 \pm i0.16$) and moving, on increasing N, toward the $N=\infty$ limiting points $\overline{\beta}=0.321\,62(1\pm i)$. In Table II such singularities are reported for some values of N. The singularity closest to the origin determines the convergence radius of the corresponding strong-coupling series. For example, for $N=3$ the strong-coupling convergence radius turns out to be $\beta_r \simeq 0.61$, which corresponds to a quite large correlation length $\xi \simeq 65$. We recall that the partition function on the square lattice has the symmetry $\beta \rightarrow -\beta$, which must also be realized in the locations of its complex singularities.

By rotation invariance the ratio $r \equiv M_s^2/M_d^2$ should go to 1 in the continuum limit. Therefore the analysis of such a ratio should be considered as a test of the procedure employed to estimate continuum physical quantities. In the large-N limit $r=1$ at all values of β. This is not true anymore at finite N, where the strong-coupling series of M_s^2 and M_d^2 differ from each other, as shown in Appendix D. From $G(x)$ up to $O(\beta^{21})$ we could calculate the ratio r up to $O(\beta^{14})$. The results of our analysis of the series of r for $N=3$ are summarized in Table III. There we report the values of the PA's and Dln-PA's of the E series at $E=1$, and those of the β series at $\beta=0.55$, which corresponds to a reasonably large correlation length $\xi \simeq 25$. We considered PA's and Dln-PA's with $l+m \geq 11$ and $m \geq l \geq 5$. The most precise determinations of r^*, the value of r at the continuum limit, come from Dln-PA's, whose final estimates are $r^* = 1.0000(12)$ from the E approximants, and $r^* = 1.0002(6)$ from the β approximants (at $\beta=0.55$). The precision of these results is remarkable.

For all $N \geq 3$ the violation of rotation invariance in the large-distance behavior of $G(x)$, monitored by the ratio μ_s/μ_d, turns out quantitatively very close to that at $N=\infty$ when considered as a function of ξ_G (in a plot the $N=3$ curve of μ_s/μ_d versus ξ_G as obtained from the strong-coupling analysis would be hardly distinguishable from the exact $N=\infty$ one). μ_s/μ_d is 1 within about 1 per mille already at $\xi \simeq 4$.

TABLE III. Analysis of the 14th order strong-coupling series of $r \equiv M_s^2/M_d^2$ for $N=3$ on the square lattice, expressed in powers of E and β. The first two lines report the values of the $[l/m]$ PA's and Dln-PA's (DLPA's) at $E=1$. The last two lines report the values of $[l/m]$ PA's and Dln-PA's at $\beta=0.55$ corresponding to $\xi \simeq 25$. We show data for PA's and Dln-PA's with $l+m \geq 11$ and $m \geq l \geq 5$. Asterisks mark defective PA's, i.e., PA's with spurious singularities close to the real axis for $E \lesssim 1$ in the energy series case, or for $\beta \lesssim 0.55$ in the β series case.

		5/6	6/6	5/7	6/7	5/8	7/7	6/8	5/9
$E=1$	PA	*	0.9965	0.9967	0.9955	1.0126	0.9980	1.0007	1.0120
	DLPA	1.0002	1.0011	1.0023	1.0005	0.9995			
$\beta=0.55$	PA	0.9986	0.9996	1.0015	1.0007	1.0010	1.0007	1.0007	1.0012
	DLPA	0.9996	1.0007	0.9993	1.0006	0.9999			

TABLE IV. Analysis of the 16th order strong-coupling series of $s \equiv M_s^2/M_G^2$ for $N=3$ on the square lattice. The first two lines report the values of the $[l/m]$ PA's and Dln-PA's at $E=1$. The last two lines report the values of $[l/m]$ PA's and Dln-PA's at $\beta=0.55$. We show data for PA's and Dln-PA's with $l+m \geq 13$ and $m \geq l \geq 5$. Asterisks mark defective PA's.

		6/7	5/8	7/7	6/8	5/9	7/8	6/9	5/10	8/8	7/9	6/10	5/11
$E=1$	PA	0.9947	0.9938	0.9941	0.9942	*	0.9944	1.0020	*	0.9961	1.0028	1.0028	*
	DLPA	0.9941	0.9971	*	0.9992	0.9978	0.9951	0.9973	0.9984				
$\beta=0.55$	PA	*	0.9971	0.9972	0.9974	*	0.9976	0.9988	0.9998	0.9980	1.0023	0.9996	0.9995
	DLPA	0.9971	0.9980	0.9974	0.9992	0.9985	0.9977	0.9982	0.9976				

Calculating a few more components of $G(x)$ at larger orders [i.e., those involved in the wall-wall correlation function at distances 6 and 7, respectively, up to $O(\beta^{22})$ and $O(\beta^{23})$], we computed the ratio

$$s \equiv \frac{M_s^2}{M_G^2} \qquad (70)$$

up to $O(\beta^{16})$, by applying the technique described in Refs. [14,15]. We recall that at $N=\infty$ we found $s=1$ independently of β. No exact results are known about the continuum limit s^* of the ratio s, except for its large-N limit: $s^*=1$. Both large-N and Monte Carlo estimates indicate a value very close to 1. From a $1/N$ expansion [16,17]:

$$s^* = 1 - \frac{0.006\,450}{N} + O\left(\frac{1}{N^2}\right). \qquad (71)$$

Monte Carlo simulations at $N=3$ [18] gave $s=0.9988(16)$ at $\beta=1.7/3=0.5666\ldots$ $(\xi \simeq 35)$, and $s=0.9982(18)$ at $\beta=0.6$ $(\xi \simeq 65)$, leading to the estimate $s^*=0.9985(12)$.

In Table IV we report, for $N=3$, the values of PA's and Dln-PA's of the energy and β series of s, respectively, at $E=1$ and at $\beta=0.55$. We considered PA's and Dln-PA's with $l+m \geq 13$ and $m \geq l \geq 5$. Combining PA and Dln-PA results, our final estimates are $s^*=0.998(3)$ from the E approximants, and $s^*=0.998(1)$ from the β approximants evaluated at $\beta=0.55$, in full agreement with the estimates from the $1/N$ expansion and Monte Carlo simulations. With increasing N, the central estimate of s^* tends to be closer to 1.

The scaling-violation pattern of the quantity μ_s/M_G for $N=3$ is similar to the pattern for $N=\infty$ [cf. Eq. (27)]; i.e., it is stable within a few per mille for $\xi \gtrsim 5$.

Another dimensionless renormalization-group-invariant quantity we have considered is $u \equiv m_2^2/(\chi m_4)$, whose large-$N$ limit has been calculated in the previous section [cf. Eq. (21)]. At finite N its continuum limit u^* is not known. From the expression of the self-energy calculated up to $O(1/N)$, [16,17,19] one can obtain

$$u^* = \frac{1}{4}\left[1 - \frac{0.006\,198}{N} + O\left(\frac{1}{N^2}\right)\right]. \qquad (72)$$

It is interesting to notice that the $O(1/N)$ correction in Eqs. (71) and (72) is very small.

At $N=3$ the analysis of the $O(\beta^{21})$ strong-coupling series of u detected a simple pole close to the origin at $\beta_0 = -0.085\,545$ for the β series, and at $E_0 = -0.086\,418$ for the energy series, corresponding to $M_G^2 = -16.000$, which, within the precision of our strong-coupling estimate, is also the location of the pole in the corresponding $N=\infty$ expression (21). Being a simple pole, this singularity can be perfectly reproduced by a standard PA analysis, and, indeed, we found PA's to be slightly more stable than Dln-PA's in the analysis of u. The results concerning $N=3$, reported in Table V (for PA's with $l+m \geq 16$ and $m \geq l \geq 8$), lead to the estimates $u^*=0.2498(6)$ from the energy analysis, and $u^*=0.2499(5)$ from the β analysis (at $\beta=0.55$). The agreement with the large-N formula (72) is satisfactory. In Fig. 2 the curve $u(E)$ as obtained from the $[10/10]$ PA and the exact curve $u(E)$ at $N=\infty$ [cf. Eq. (21)] are plotted, showing almost no differences.

In Table VI we give a summary of the determinations of r^*, s^*, and u^* from PA's and Dln-PA's of the energy and β series.

We mention that we also tried to analyze series in the variable

TABLE V. Analysis of the 20th order strong-coupling series of $E^{-1}u(E)$ and $\beta^{-1}u(\beta)$, where $u \equiv m_2^2/(\chi m_4)$, for $N=3$ on the square lattice. The first two lines report the values of u as obtained from the $[l/m]$ PA's and Dln-PA's at $E=1$. The last two lines report the values of u from $[l/m]$ PA's and Dln-PA's at $\beta=0.55$. The analysis detected a pole at $E_0 = -0.086\,418$ in the energy series, and at $\beta_0 = -0.085\,545$ in the β series, corresponding to $M_G^2 = -16.000$. We show data for PA's and Dln-PA's with $l+m \geq 16$ and $m \geq l \geq 8$. Asterisks mark defective approximants.

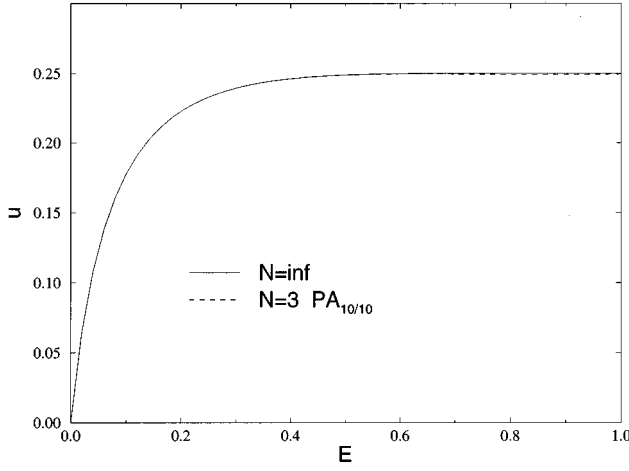|		8/8	8/9	9/9	9/10	8/11	10/10	9/11	8/12
$E=1$	PA	0.2491	0.2502	0.2495	0.2488	0.2491	0.2495	0.2504	0.2496
	DLPA	0.2497	0.2524	0.2510	0.2486	0.2492			
$\beta=0.55$	PA	0.2493	0.2496	0.2488	0.2496	0.2500	*	0.2495	0.2503
	DLPA	0.2493	0.2495	0.2491	0.2498	0.2500			

FIG. 2. $u \equiv m_2^2/(\chi m_4)$ versus E for $N=3$ (as obtained by the [10/10] PA) and $N=\infty$ (exact), on the square lattice.

$$z = \frac{I_{N/2}(N\beta)}{I_{N/2-1}(N\beta)}, \qquad (73)$$

which is the character coefficient of the fundamental representation. As for the E series, the continuum limit should be reached at a finite value $z \to 1$, and estimates of r^*, s^*, and u^* may be obtained by evaluating the approximants of the corresponding z series at $z=1$. We obtained results much less precise than those from the analysis of the E series. Maybe because of the thermodynamical meaning of the internal energy, resummations by PA's and Dln-PA's of the E series turn out much more effective, providing rather precise results even at the continuum limit $E=1$.

The strong-coupling approach turns out to be less effective for the purpose of checking asymptotic scaling. In Table VII, we compare, for $N=3$, 4, and 8, ξ_G as obtained from the plain 21st order series of ξ_G^2 and from its Dln-PA's with some Monte Carlo results available in the literature. Resum-

TABLE VI. In this table we summarize our strong-coupling results for $N=3$, giving the estimates of r^*, s^*, and u^* from the PA and Dln-PA analyses of both the energy and β-series of r, s, and u. For all lattices considered the values of β where the β approximants have been evaluated correspond to a correlation length $\xi \gtrsim 20$.

			r^*	s^*	u^*
Square	$E=1$	PA	1.004(8)	1.000(5)	0.2498(6)
		DLPA	1.0000(12)	0.997(2)	0.249(2)
	$\beta=0.55$	PA	1.0009(6)	1.000(2)	0.2499(6)
		DLPA	1.0002(6)	0.9978(8)	0.2499(5)
Triangular	$E=1$	PA		1.000(4)	0.2497(15)
		DLPA		0.997(3)	0.248(2)
	$\beta=0.33$	PA		0.9985(13)	0.2504(3)
		DLPA		0.9980(9)	0.2499(4)
Honeycomb	$E=1$	PA	1.01(4)	0.999(4)	0.250(2)
		DLPA	0.991(13)	0.999(3)	0.247(2)
	$\beta=0.85$	PA	1.001(2)	0.9987(5)	0.2490(3)
		DLPA	1.0009(8)	0.9987(5)	0.2491(3)

TABLE VII. The strong-coupling estimates of ξ_G are compared with the available Monte Carlo results on the square lattice for various values of N. The strong-coupling estimates of ξ_G come from the plain series of ξ_G^2, and from ([9/10],[8/11],[9/9],[8/10]) Dln-PA's of $\beta^{-1}\xi_G^2$. The $N=3,4,8$ Monte Carlo (MC) data are taken, respectively, from Refs. [28,29], and [24]. The asterisk indicates that the number concerns $\xi_{\exp}$, and not ξ_G.

N	β	Plain series	Dln-PA's	MC
3	1.4/3	6.567	6.869(1)	6.90(1)*
	0.5	9.939	11.036(4)	11.05(1)*
	1.6/3	15.429	18.90(2)	19.00(2)*
	1.7/3	24.300	33.9(1)	34.44(6)*
	0.6	38.459	61.0(4)	64.7(3)*
4	0.45	4.665	4.672(1)	4.67(1)
	0.5	7.845	7.87(1)	7.83(1)
	0.55	13.879	13.88(5)	13.99(3)
	0.575	18.701	18.6(2)	18.91(5)
	0.6	25.329	24.8(4)	25.5(2)
8	0.5	5.432	5.459(1)	5.461(5)*
	0.525	6.584	6.651(1)	
	0.55	7.981	8.139(2)	
	0.575	9.659	10.01(1)	9.884(13)*

mation by integral approximants [20] provides results substantially equivalent to those of Dln-PA's. For $N=3$ Dln-PA's follow Monte Carlo data reasonably well up to about the convergence radius $\beta_r \simeq 0.6$ of the strong-coupling expansion, but they fail beyond β_r. On the other hand, it is well known that for $N=3$ the asymptotic scaling regime is set at larger β values [21]. More sophisticated analyses can be found in Refs. [11,22], but they do not seem to lead to a conclusive result about the asymptotic freedom prediction in the O(3) σ model. At larger N, the convergence radius decreases, but on the other hand the asymptotic scaling regime should be reached earlier. At $N=4$ and $N=8$ the 21st order plain series of ξ_G^2 provides already quite good estimates of ξ_G within the convergence radius when compared with Monte Carlo results. Again, Padé-type resummation fails for $\beta > \beta_r$. We mention that at $N=4$ the convergence radius $\beta_r \simeq 0.60$ corresponds to $\xi_G \simeq 25$, and at $N=8$ $\beta_r \simeq 0.55$ corresponds to $\xi_G \simeq 8$.

In order to check asymptotic scaling we consider the ratio Λ_s/Λ_{2l}, where Λ_s is the effective Λ parameter which can be extracted by

$$\Lambda_s \equiv \left(\frac{\Lambda_s}{M}\right) M = \frac{M}{R_s}, \qquad (74)$$

where M is an estimator of the mass gap, R_s is the mass-Λ parameter ratio in the square lattice nearest-neighbor formulation [23],

$$R_s = R_{\overline{MS}} \times \left(\frac{\Lambda_{\overline{MS}}}{\Lambda_s}\right)$$

$$= \left(\frac{8}{e}\right)^{1/(N-2)} \frac{1}{\Gamma(1+1/(N-2))} \sqrt{32} \exp\left[\frac{\pi}{2(N-2)}\right], \qquad (75)$$
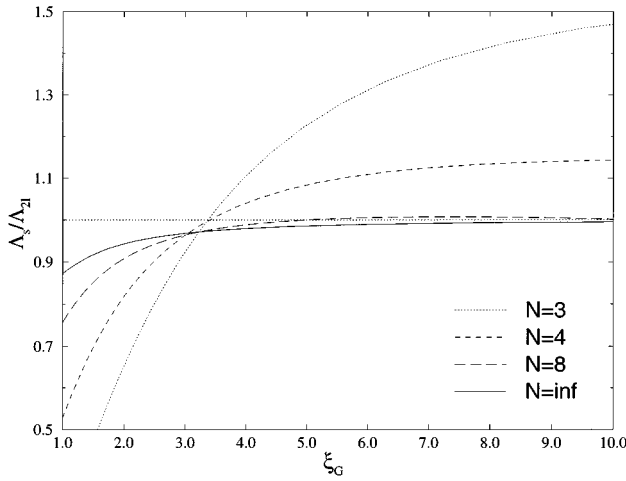
FIG. 3. Asymptotic scaling test from the strong-coupling determinations of ξ_G^2 on the square lattice. We show curves of Λ_s/Λ_{2l}, defined by Eqs. (75) and (76), for $N=3,4,8$, and for $N=\infty$ (exact).

where $\overline{\text{MS}}$ denotes the modified minimal substraction scheme and Λ_{2l} is the corresponding two-loop formula

$$\Lambda_{2l}=\left(\frac{2\pi N}{N-2}\beta\right)^{1/(N-2)}\exp\left(-\frac{2\pi N}{N-2}\beta\right). \qquad (76)$$

The ratio Λ_s/Λ_{2l} should go to 1 in the continuum limit, according to asymptotic scaling. The available series of M_G^2 are longer than any series of the mass-gap estimators; therefore, neglecting the very small difference between M_G and M [we have seen that for $N\geq 3$ $(M_G-M)/M\lesssim 10^{-3}$ in the continuum limit], for which formula (75) holds, we use M_G as estimator of M. In Fig. 3 we plot Λ_s/Λ_{2l} for various values of N, $N=3,4,8$, and for comparison the exact curve for $N=\infty$. As already noted in Ref. [24] by a Monte Carlo study, for $N=3,4$ at $\xi\simeq 10$ the asymptotic scaling regime is still far away (about 50% off at $N=3$ and 15% at $N=4$), while for $N=8$ it is verified for $\xi\gtrsim 4$ within a few percent. Notice also that the convergence radius $\beta_r\simeq 0.55$ corresponds to $\xi\simeq 8$. Anyway, with increasing N curves of Λ_s/Λ_{2l} clearly approach the exact $N=\infty$ limit.

C. The triangular lattice

On the triangular lattice we have calculated the two-point Green's function up to $O(\beta^{15})$, from which we have extracted strong-coupling series of the quantities E, χ, ξ_G^2,

u, and M_t^2, already introduced in Sec. II C, and of the ratios $s\equiv M_t^2/M_G^2$. Some of the above series for $N=3$ are reported in Appendix E.

Like $O(N)$ σ models on the square lattice, no indication of the presence of a critical point at a finite real value of β emerges from the strong-coupling analysis for $N\geq 3$. By a Dln-PA analysis of the $O(\beta^{15})$ strong-coupling series of χ and ξ_G^2 at $N=3$, we found that the singularity closest to the origin is $\overline{\beta}\simeq 0.358\pm i0.085$, giving rise to a convergence radius $\beta_r\simeq 0.37$ which should correspond to a rather large correlation length: $\xi_G\simeq 70$. On increasing N, such singularities move toward their $N=\infty$ limit $\overline{\beta}=0.206\,711\pm i\,0.181\,627$. Some details of this analysis are given in Table II.

In our analysis of dimensionless quantities we considered, as on the square lattice, the series both in the energy and in β. The estimates concerning the continuum limit are obtained by evaluating the approximants of the energy series at $E=1$, and those of the β series at a β associated with a reasonably large correlation length. For $N=3$ we chose $\beta=0.33$, whose corresponding correlation length should be $\xi\simeq 22$, according to a strong-coupling estimate.

Calculating a few more components of $G(x)$ at larger orders [i.e., those involved in the wall-wall correlation function at distance $\sqrt{3}/2\times 5$ up to $O(\beta^{16})$], we computed the ratio $s\equiv M_t^2/M_G^2$ up to $O(\beta^{11})$ [14,15]. For $N=3$ the analysis of the strong-coupling series of s (some details are given in Table VIII) leads to the estimate $s^*=0.998(3)$ from the energy approach, and $s^*=0.998(1)$ evaluating the approximants at $\beta=0.33$ (we considered PA's and Dln-PA's with $l+m\geq 8$ and $m\geq l\geq 4$). Such results are in perfect agreement with those found for the square lattice.

PA's and Dln-PA's (with $l+m\geq 11$ and $m\geq l\geq 5$) of the strong-coupling series of u expressed in terms of the energy, evaluated at $E=1$, lead to the estimate $u^*=0.249(1)$ at $N=3$. The analysis of the series in β gives $u^*=0.2502(4)$. Again universality is satisfied.

A summary of the results on the triangular lattice can be found in Table VI.

As on the square lattice we checked asymptotic scaling by looking at the ratio Λ_t/Λ_{2l}, where Λ_t is the effective Λ parameter on the triangular lattice, defined in analogy with Eq. (74). In addition to the formulas concerning asymptotic scaling given for the square lattice case [cf. Eqs. (74)-(76)], we need here the Λ-parameter ratio Λ_t/Λ_s calculated in Appendix A, [cfr. Eq. (A13)]. We again used M_G as approximate estimator of the mass gap M. Figure 4 shows curves of Λ_t/Λ_{2l} for various values of N, $N=3,4,8$, and for comparison the exact curve for $N=\infty$. Such results are similar to

TABLE VIII. Analysis of the 11th order strong-coupling series of $s\equiv M_t^2/M_G^2$ for $N=3$ on the triangular lattice. The first two lines report the values of the $[l/m]$ PA's and Dln-PA's at $E=1$. The last two lines report the values of $[l/m]$ PA's and Dln-PA's at $\beta=0.33$ corresponding to $\xi\simeq 22$. Asterisks mark defective PA's.

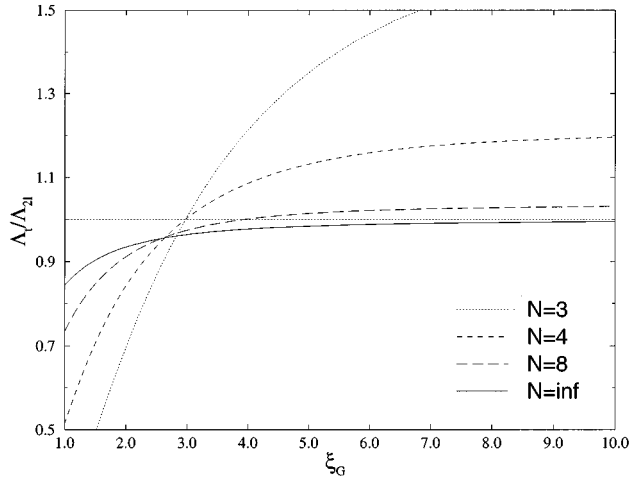|		4/4	4/5	5/5	4/6	5/6	4/7
$E=1$	PA	0.9993	0.9972	1.0005	0.9927	0.9954	1.0039
	DLPA	0.9963	1.0014	0.9948	*		
$\beta=0.33$	PA	0.9993	0.9989	1.0005	0.9969	0.9974	0.9995
	DLPA	0.9987	*	0.9972	0.9975		

FIG. 4. Asymptotic scaling test from the strong-coupling determinations of ξ_G^2 on the triangular lattice. Curves of Λ_t/Λ_{2l} for $N=3,4,8$ and for $N=\infty$ (exact) are shown vs ξ_G.

those found on the square lattice: for $N=3,4$ the asymptotic scaling regime is still far away at $\xi_G \simeq 10$, but it is verified within a few percent at $N=8$, where the correlation length corresponding to the strong-coupling convergence radius is $\xi \simeq 8$.

D. The honeycomb lattice

On the honeycomb lattice we have calculated the two-point Green's function up to $O(\beta^{30})$, from which we extracted strong-coupling series of the quantities E, χ, ξ_G^2, u, M_v^2, and M_h^2, already introduced in Sec. II D, and of the ratios $r \equiv M_v^2/M_h^2$ and $s \equiv M_h^2/M_G^2$. Some of the above series for $N=3$ are reported in Appendix F.

At $N=3$ a Dln-PA analysis of the $O(\beta^{30})$ strong-coupling series of χ and ξ_G^2 detected two couples of complex conjugate singularities, one on the imaginary axis at $\bar{\beta} \simeq \pm i0.460$, quite close to the origin, and the other at $\bar{\beta} \simeq 0.93 \pm i0.29$. The singularity on the imaginary axis leads to a rather small convergence radius in terms of correlation length; indeed, at $\beta \simeq 0.46$ we estimate $\xi \simeq 2.6$. At $N=4$ we found $\bar{\beta} \simeq \pm i0.444$, and $\bar{\beta} \simeq 0.88 \pm i0.41$. At larger N the singularities closest to the origin converge toward the $N=\infty$ value $\bar{\beta} = \pm i\, 0.362\,095$. Notice that, as on the square lattice, the partition function on the honeycomb lattice enjoys the symmetry $\beta \to -\beta$.

Again we analyzed the series both in the energy and in β. The estimates concerning the continuum limit are obtained by evaluating the approximants of the energy series at $E=1$, and those of the β series at $\beta=0.85$ for the $N=3$ case, which should correspond to $\xi \simeq 22$.

By rotation invariance the ratio $r \equiv M_h^2/M_v^2$ should go to 1 in the continuum limit. From $G(x)$ up to $O(\beta^{30})$ we extracted the ratio r up to $O(\beta^{20})$. Again, PA's and Dln-PA's of the energy series evaluated at $E=1$ and of the β series evaluated at $\beta=0.85$ (some details are given in Table X) give the correct result in the continuum limit: respectively, $r^*=1.00(1)$ and $r^*=1.001(1)$ at $N=3$ (we considered PA's and Dln-PA's with $l+m \geq 16$ and $m \geq l \geq 7$).

Calculating a few more components of $G(x)$ at larger orders [i.e., those involved in $G_h^{(w)}(x)$, defined in Eq. (B7), at distances $x=\sqrt{3}/2 \times 9$ and $x=\sqrt{3}/2 \times 10$, respectively, at $O(\beta^{34})$ and $O(\beta^{35})$], we computed the ratio $s \equiv M_h^2/M_G^2$ up to $O(\beta^{25})$ [14,15]. For $N=3$ the analysis of the strong-coupling series of s gives $s^*=0.999(3)$ from the E approximants and $s^*=0.9987(5)$ from the β approximants evaluated at $\beta=0.85$ (some details are given in Table XI), in agreement with the result found on the other lattices. We considered PA's and Dln-Pa's with $l+m \geq 22$ and $m \geq l \geq 10$.

The analysis of the energy series of u confirms universality: PA's and Dln-PA's (with $l \leq m$, $l+m \geq 26$, $l \geq 12$) of the energy series evaluated at $E=1$ give $u^*=0.249(3)$, and those of the β series at $\beta=0.85$ and $u^*=0.2491(3)$. As for the square lattice, the curve $u(E)$ obtained from the PA's at $N=3$ and the exact curve $u(E)$ at $N=\infty$ [cf. Eq. (60)], would be hardly distinguishable if plotted together.

As noted above, the convergence radius β_r is small in terms of the correlation length for all values of N: it goes from $\xi \simeq 1.0$ at $N=\infty$ to $\xi \simeq 2.6$ at $N=3$. Nevertheless, in this case Dln-PA resummations seem to give reasonable estimates of ξ_G even beyond β_r (apparently up to about the next singularity closest to the origin). In Fig. 5 we show curves of Λ_h/Λ_{2l}, where Λ_h is the effective Λ parameter on the honeycomb lattice, for various values of N, $N=3,4,8$, and for comparison the exact curve for $N=\infty$. The necessary ratio of Λ parameters has been calculated in Appendix B [cf. Eqs. (B11) and (B12)].

E. Conclusions

We have shown that quite accurate continuum limit estimates of dimensionless renormalization-group-invariant

TABLE IX. Analysis of the 14th order strong-coupling series of $E^{-1}u(E)$ and $\beta^{-1}u(\beta)$, where $u \equiv m_2^2/(\chi m_4)$, for $N=3$ on the triangular lattice. The first two lines report the values of u as obtained from the $[l/m]$ PA's and Dln-PA's at $E=1$. The last two lines report the values of u from $[l/m]$ PA's and Dln-PA's at $\beta=0.33$ corresponding to $\xi \simeq 22$. A pole has been detected at $E_0 = -0.050\,655$, corresponding to $M_G^2 = -16.000$. Asterisks mark defective PA's.

		5/6	6/6	5/7	6/7	5/8	7/7	6/8	5/9
$E=1$	PA	0.2442	0.2502	0.2533	0.2483	0.2492	0.2494	0.2500	0.2497
	DLPA	0.2433	0.2521	0.2502	0.2477	0.2491			
$\beta=0.33$	PA	0.2521	0.2500	0.2500	0.2502	0.2502	0.2504	0.2505	0.2502
	DLPA	0.2496	0.2494	0.2494	0.2496	0.2502			

TABLE X. Analysis of the 19th order strong-coupling series of r/β, where $r \equiv M_h^2/M_v^2$, for $N=3$ on the honeycomb lattice, expressed in powers of E and β. The first two lines report the values of the $[l/m]$ PA's and Dln-PA's at $E=1$. The last two lines report the values of $[l/m]$ PA's and Dln-PA's at $\beta=0.85$ corresponding to $\xi \simeq 22$. Asterisks mark defective PA's, i.e., PA's with spurious singularities close to the real axis for $E \lesssim 1$ in the energy series case, or for $\beta \lesssim 0.85$ in the β series case.

		8/8	7/9	8/9	7/10	9/9	8/10	7/11	9/10	8/11	7/12
$E=1$	PA	1.070	0.963	1.006	1.035	*	0.981	1.035	0.980	0.980	1.080
	DLPA	1.007	0.996	0.977	1.010	0.993	0.989	*			
$\beta=0.85$	PA	1.0039	*	1.0020	1.0031	*	0.9988	*	0.9996	0.9997	1.0024
	DLPA	1.0006	0.9992	1.0019	1.0009	1.0009	1.0014	1.0005			

quantities, such as s and u [cfr. Eqs. (70) and (21)], can be obtained by analyzing their strong-coupling series and applying resummation techniques both in the inverse temperature variable β and in the energy variable E. In particular, in order to get continuum estimates from the analysis of the energy series, we evaluated the corresponding PA's and Dln-PA's at $E=1$, i.e., at the continuum limit. This idea has already been applied to the calculation of the continuum limit of the zero-momentum four-point coupling g_r, obtaining accurate results [6]. These results look very promising in view of a possible application of such strong-coupling analysis to four-dimensional gauge theories.

The summary in Table VI of our $N=3$ strong-coupling results for the continuum values r^*, s^*, and u^*, for all lattices we have considered, shows that universality is verified within a precision of a few per mille, leading to the final estimates $s^* \simeq 0.9985$ and $u^* \simeq 0.2495$ with an uncertainty of about 1 per mille. The comparison with the exact $N=\infty$ results, $s^*=1$ and $u^*=1/4$, shows that quantities like s^* and u^*, which describe the small-momentum universal behavior of $\widetilde{G}(p)$ in the continuum limit, change very little and apparently monotonically from $N=3$ to $N=\infty$, suggesting that at $N=3$ $\widetilde{G}(p)$ is essentially Gaussian at small momentum.

Let us make this statement more precise. In the critical region one can expand the dimensionless renormalization-group-invariant function

$$L(p^2/M_G^2) \equiv \frac{\widetilde{G}(0)}{\widetilde{G}(p)} \tag{77}$$

around $y \equiv p^2/M_G^2 = 0$, writing

$$L(y) = 1 + y + l(y),$$

$$l(y) = \sum_{i=2}^{\infty} c_i y^i. \tag{78}$$

$l(y)$ parametrizes the difference from a generalized Gaussian propagator. One can easily relate the coefficients c_i of the expansion (78) to dimensionless renormalization-group-invariant ratios involving the moments m_{2j} of $G(x)$.

It is worth observing that

$$u^* = \frac{1}{4(1-c_2)}. \tag{79}$$

In the large-N limit the function $l(y)$ is depressed by a factor $1/N$. Moreover, the coefficients of its low-momentum expansion are very small. They can be derived from the $1/N$ expansion of the self-energy [16,17,19]. In the leading order in the $1/N$ expansion one finds

$$c_2 \simeq -\frac{0.006\,198\,16\ldots}{N},$$

$$c_3 \simeq \frac{0.000\,238\,45\ldots}{N},$$

$$c_4 \simeq -\frac{0.000\,013\,44\ldots}{N},$$

$$c_5 \simeq \frac{0.000\,000\,90\ldots}{N}, \tag{80}$$

etc. For sufficiently large N we then expect

$$c_i \ll c_2 \ll 1 \quad \text{for} \quad i \geq 3. \tag{81}$$

As a consequence, since the zero of $L(y)$ closest to the origin is $y_0 = -s^*$, the value of s^* is substantially fixed by the term proportional to $(p^2)^2$ in the inverse propagator, through the approximate relation
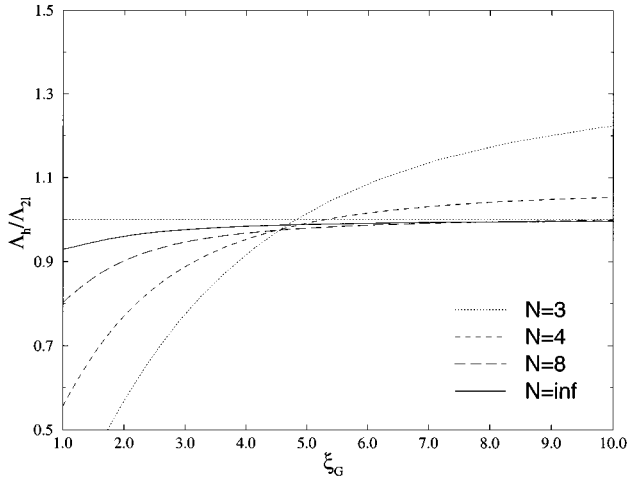
$$s^* - 1 \simeq c_2 \simeq 4u^* - 1. \tag{82}$$

TABLE XI. Analysis of the 25th order strong-coupling series of $s \equiv M_h^2/M_G^2$ for $N=3$ on the honeycomb lattice. The first two lines report the values of the $[l/m]$ PA's and Dln-PA's at $E=1$. The last two lines report the values of $[l/m]$ PA's and Dln-PA's at $\beta=0.85$ corresponding to $\xi \simeq 22$. Asterisks mark defective PA's.

		11/11	10/12	11/12	10/13	12/12	11/13	10/14	12/13	11/14	10/15
$E=1$	PA	0.9956	1.0001	1.0052	0.9983	*	*	*	*	*	*
	DLPA	*	0.9964	0.9994	0.9963	1.0023	*	0.9972			
$\beta=0.85$	PA	0.9978	0.9984	0.9983	0.9982	*	0.9983	0.9991	0.9982	0.9989	0.9989
	DLPA	0.9989	0.9982	*	0.9982	*	0.9992	0.9983			

FIG. 5. Asymptotic scaling test from the strong-coupling determinations of ξ_G^2 on the honeycomb lattice. Curves of Λ_h/Λ_{2l} for $N=3,4,8$ and for $N=\infty$ (exact) are shown vs ξ_G.

Indeed, in the large-N limit one finds, from Eqs. (71) and (72),

$$s^*-4u^*=\frac{-0.000\,252}{N}+O\!\left(\frac{1}{N^2}\right), \tag{83}$$

where the coefficient of the $1/N$ term is much smaller than those of s^* and u^*.

From this large-N analysis one expects that even at $N=3$ the function $l(y)$ will be small in a relatively large region around $y=0$. This is confirmed by the strong-coupling estimate of u^*, which, using Eq. (79), leads to $c_2\simeq-0.002$. Furthermore, the comparison of the estimates of s^* and u^* shows that $s^*-4u^*\simeq0$ within the precision of our analysis, consistently with Eq. (81). It is interesting to note that similar results have been obtained for the models with $N\leq2$, and in particular for the Ising model, i.e., for $N=1$, where the strong-coupling analysis turns out to be very precise [2].

We can conclude that the two-point Green's function for all $N\geq3$ is almost Gaussian in a large region around $p^2=0$, i.e., $|p^2/M_G^2|\lesssim1$, and the small corrections to Gaussian behavior are essentially determined by the $(p^2)^2$ term in the expansion of the inverse propagator.

Differences from Gaussian behavior will become important at sufficiently large momenta, as predicted by simple weak-coupling calculations supplemented by a renormalization-group resummation. Indeed, the asymptotic behavior of $G(x)$ for $x\ll1/M$ (where M is the mass gap) turns out to be

$$G(x)\sim\left(\ln\frac{1}{xM}\right)^{\gamma_1/b_0},\qquad\frac{\gamma_1}{b_0}=\frac{N-1}{N-2}; \tag{84}$$

b_0 and γ_1 are the first coefficients of the β function and of the anomalous dimension of the fundamental field $\vec{s}$, respectively. Let us recall that a free Gaussian Green's function behaves like $\ln(1/x)$. Important differences are present in other Green's functions even at small momentum, as shown in the analysis of the four-point zero-momentum renormal-

ized coupling, whose definition involves the zero-momentum four-point correlation function (34) [6]. However, monotonicity in N seems to be a persistent feature.

Our strong-coupling calculations allow also a check of asymptotic scaling for a relatively large range of correlation lengths. For all lattices considered, the ratio between the effective Λ parameter extracted from the mass gap and its two-loop approximation Λ/Λ_{2l}, when considered as a function of ξ_G, shows similar patterns with changing N. Confirming earlier Monte Carlo studies, large discrepancies from asymptotic scaling are observed for $N=3$ in the range of correlation lengths we could reliably investigate, i.e., $\xi\lesssim50$. At $N=8$ and for all lattices considered, asymptotic scaling within a few percent is verified for $\xi\gtrsim4$, and on increasing N the ratio Λ/Λ_{2l} smoothly approaches its $N=\infty$ limit.

ACKNOWLEDGMENTS

APPENDIX A: THE TRIANGULAR LATTICE

The sites $\vec{x}$ of a finite periodic triangular lattice can be represented in Cartesian coordinates by

$$\vec{x}(l_1,l_2)=l_1\vec{\eta}_1+l_2\vec{\eta}_2,$$

$$l_1=1,\ldots,L_1,\qquad l_2=1,\ldots,L_2,$$

$$\vec{\eta}_1=(1,0),\qquad\vec{\eta}_2=\left(\frac{1}{2},\frac{\sqrt{3}}{2}\right). \tag{A1}$$

We set $a=1$, where the lattice space a is the length of a link. The total number of sites, links, and triangles is, respectively, $N_s=L_1L_2$, $N_l=3N_s$, and $N_t=2N_s$. Taking into account periodic boundary conditions, a finite lattice Fourier transform can be defined by

$$\phi(\vec{k})=\sum_{\vec{x}}e^{i\vec{k}\cdot\vec{x}}\phi(\vec{x}),$$

$$\phi(\vec{x})=\frac{1}{v_sN_s}\sum_{\vec{k}}e^{i\vec{k}\cdot\vec{x}}\phi(\vec{k}), \tag{A2}$$

where $v_s=\sqrt{3}/2$ is the volume per site, and the set of momenta is

$$\vec{k}(m_1,m_2)=\frac{2\pi}{L_1}m_1\vec{\rho}_1+\frac{2\pi}{L_2}m_2\vec{\rho}_2,$$

$$m_1=1,\ldots,L_1,\qquad m_2=1,\ldots,L_2,$$

$$\vec{\rho}_1=\left(1,-\frac{1}{\sqrt{3}}\right),\qquad\vec{\rho}_2=\left(0,\frac{2}{\sqrt{3}}\right). \tag{A3}$$

Notice that

$$\vec{k} \cdot \vec{x} = \frac{2\pi}{L_1} m_1 l_1 + \frac{2\pi}{L_2} m_2 l_2. \qquad \text{(A4)}$$

To begin with, let us discuss the Gaussian model on the triangular lattice, which is defined by the action

$$S_G = \frac{\kappa}{2} \sum_{\text{links}} (\phi_{x_l} - \phi_{x_r})^2 \qquad \text{(A5)}$$

where x_l and x_r indicate the sites at the ends of each link. Performing the Fourier transform (A2) one derives the propagator

$$\langle \phi(k) \phi(q) \rangle = \frac{v_s}{\sqrt{3}\kappa} \frac{1}{\Delta(k)} \delta_{k+q,0},$$

$$\Delta(k) = 4 \left[1 - \frac{1}{3} \left(\cos k_1 + 2\cos\frac{k_1}{2}\cos\frac{\sqrt{3}k_2}{2} \right) \right]. \qquad \text{(A6)}$$

From these formulas one can easily obtain the large-N limit, since the model becomes Gaussian for $N \to \infty$.

In the massive Gaussian model one may define an exponentiated wall-wall correlation function by

$$G_t^{(w)}\left(\frac{\sqrt{3}}{2} l_2 \right) = \sum_{l_1} G(l_1 \vec{\eta}_1 + l_2 \vec{\eta}_2). \qquad \text{(A7)}$$

In the $O(N)$ σ models, in order to evaluate the ratio between the Λ parameter of the $\overline{\text{MS}}$ renormalization scheme and the triangular nearest-neighbor lattice regularization, we calculated the correlation function $G(x)$ in perturbation theory. In the x space we obtained [neglecting $O(a^2)$ terms]

$$G(x) = 1 + \frac{N-1}{N} tF(a/x) + O(t^2),$$

$$F(a/x) = \frac{1}{2\pi} \left(\ln\frac{a}{x} - \gamma_E - \ln 2 - \frac{1}{2}\ln 3 \right). \qquad \text{(A8)}$$

In the p space,

$$\widetilde{G}(k) = \frac{N-1}{N} \frac{t}{k^2} \left[1 + \frac{t}{N} \left(D(ak) + \frac{1}{2\sqrt{3}} \right) + O(t^2) \right],$$

$$D(ak) = \frac{1}{2\pi} \left(\ln ak - 2\ln 2 - \frac{1}{2}\ln 3 \right). \qquad \text{(A9)}$$

The above results required the calculation of the integral

$$\int_{-\pi}^{\pi} \frac{dk_1}{2\pi} \int_{-2\pi/\sqrt{3}}^{2\pi/\sqrt{3}} \frac{dk_2}{2\pi} \frac{e^{ikx}-1}{\Delta(k)} = F(a/x) + O(a/x),$$

$$\int_{-\pi}^{\pi} \frac{dk_1}{2\pi} \int_{-2\pi/\sqrt{3}}^{2\pi/\sqrt{3}} \frac{dk_2}{2\pi} \frac{\Delta(q) - \Delta(k) - \Delta(k+q)}{\Delta(k)\Delta(k+q)}$$

$$= 2D(aq) + O(aq), \qquad \text{(A10)}$$

where the extremes of integration are chosen to cover the appropriate Brillouin zone, which can be determined from the finite lattice momenta (A3).

Comparing the above results with the two-point Green's function renormalized in the $\overline{\text{MS}}$ scheme,

$$G_{\overline{\text{MS}}}(x\mu = 2e^{-\gamma_E}) = 1 + O(t_r^2),$$

$$\widetilde{G}_{\overline{\text{MS}}}\left(\frac{k}{\mu} = 1 \right) = \frac{N-1}{N} \frac{t_r}{k^2} [1 + O(t_r^2)], \qquad \text{(A11)}$$

and following a standard procedure, one can determine the ratio of the Λ parameters:

$$\frac{\Lambda_{\overline{\text{MS}}}}{\Lambda_t} = 4\sqrt{3}\exp\left(\frac{\pi}{(N-2)} \frac{1}{\sqrt{3}} \right), \qquad \text{(A12)}$$

where Λ_t is the Λ parameter of the $O(N)$ σ models on the triangular lattice. Furthermore, comparing with the Green's function calculated on the square lattice [25] one can also derive

$$\frac{\Lambda_s}{\Lambda_t} = \sqrt{\frac{3}{2}}\exp\left[\frac{\pi}{N-2} \left(\frac{1}{\sqrt{3}} - \frac{1}{2} \right) \right], \qquad \text{(A13)}$$

where Λ_s is the Λ parameter on the square lattice.

APPENDIX B: THE HONEYCOMB LATTICE

The sites $\vec{x}$ of a finite periodic honeycomb lattice can be represented in Cartesian coordinates by

$$\vec{x} = \vec{x}' + p\vec{\eta}_p,$$

$$\vec{x}' = l_1 \vec{\eta}_1 + l_2 \vec{\eta}_2,$$

$$l_1 = 1, \dots, L_1, \quad l_2 = 1, \dots, L_2, \quad p = 0,1,$$

$$\vec{\eta}_1 = \left(\frac{3}{2}, \frac{\sqrt{3}}{2} \right), \quad \vec{\eta}_2 = (0, \sqrt{3}), \quad \vec{\eta}_p = (1,0). \qquad \text{(B1)}$$

We set $a = 1$, where the lattice space a is the length of a link. The total number of sites, links, and hexagons is, respectively, $N_s = 2L_1 L_2$, $N_1 = 3L_1 L_2$, and $N_h = L_1 L_2$. The coordinate p can be interpreted as the parity of the corresponding lattice site: sites with the same parity are connected by an even number of links.

The two sublattices identified by $\vec{x}_+(l_1,l_2) \equiv \vec{x}(l_1,l_2,0)$ and $\vec{x}_-(l_1,l_2) \equiv \vec{x}(l_1,l_2,1)$ form a triangular lattice. Each link of the honeycomb lattice connects sites belonging to different sublattices. Triangular lattices have a more symmetric structure, in that their sites are characterized by a group of translations. It is then convenient to rewrite a field $\phi(\vec{x}) \equiv \phi(l_1,l_2,p)$ in terms of two new fields $\phi_+(\vec{x}_+) \equiv \phi(\vec{x}_+)$ and $\phi_-(\vec{x}_-) \equiv \phi(\vec{x}_-)$ defined, respectively, on the sublattices $\vec{x}_+$ and $\vec{x}_-$. Taking into account periodic boundary conditions, a finite lattice Fourier transform can be consistently defined [4]:

$$\phi_\pm(\vec{k}) = v_h \sum_{\vec{x}_\pm} e^{i\vec{k}\cdot\vec{x}_\pm} \phi_\pm(\vec{x}_\pm),$$

$$\phi_{\pm}(\vec{x}_{\pm}) = \frac{1}{v_h L_1 L_2} \sum_{\vec{k}} e^{-i\vec{k}\cdot\vec{x}_{\pm}} \phi_{\pm}(\vec{k}), \qquad \text{(B2)}$$

where $v_h = 3\sqrt{3}/2$ is the volume of a hexagon, and the set of momenta is

$$\vec{k} = \frac{2\pi}{L_1} m_1 \vec{\rho}_1 + \frac{2\pi}{L_2} m_2 \vec{\rho}_2,$$

$$m_1 = 1, \ldots, L_1, \quad m_2 = 1, \ldots, L_2,$$

$$\vec{\rho}_1 = \left(\frac{2}{3}, 0\right), \quad \vec{\rho}_2 = \left(-\frac{1}{3}, \frac{1}{\sqrt{3}}\right). \qquad \text{(B3)}$$

Using the results reported in Ref. [4] one can find the following expression for the matrix R^{-1} [cf. Eq. (13)]:

$$R^{-1}(\vec{x};\vec{y}) = R^{-1}(\vec{x}', p_x; \vec{y}', p_y)$$

$$= \frac{t}{v_s N_s} \sum_{\vec{k}} e^{i\vec{k}\cdot(\vec{x}'-\vec{y}')} \frac{1}{\Delta(k) + z(1 + \frac{1}{8}z)}$$

$$\times \begin{pmatrix} 1 + \frac{1}{4}z & e^{-ik_1}H(k)^* \\ e^{ik_1}H(k) & 1 + \frac{1}{4}z \end{pmatrix} \qquad \text{(B4)}$$

where

$$\Delta(k) = \frac{8}{9}\left[2 - \cos\frac{\sqrt{3}}{2}k_2\left(\cos\frac{3}{2}k_1 + \cos\frac{\sqrt{3}}{2}k_2\right)\right],$$

$$H(k) = e^{-ik_1}\frac{1}{3}\left(1 + 2e^{i3k_1/2}\cos\frac{\sqrt{3}}{2}k_2\right). \qquad \text{(B5)}$$

In the large-N limit $R^{-1}(x;y)$ represents the two-point Green's function.

In Ref. [14], guided by the analysis of the Gaussian model on the honeycomb lattice, two wall-wall correlation functions were defined:

$$G_v^{(w)}(\tfrac{3}{2}l_1) = \sum_{l_2} G(l_1\vec{\eta}_1 + l_2\vec{\eta}_2), \qquad \text{(B6)}$$

with the sum running over sites of positive parity forming a vertical line,

$$G_h^{(w)}(\tfrac{1}{2}\sqrt{3}l) = \sum_{l_2, p} G[(l - 2l_2)\vec{\eta}_1 + l_2\vec{\eta}_2 + p\vec{\eta}_p], \quad \text{(B7)}$$

where the sum is performed over all sites having the same coordinate x_2. $G_v^{(w)}(x)$ and $G_h^{(w)}(x)$ allow the definition of two estimators of the mass gap, μ_v and μ_h, whose ratio must go to 1 in the continuum limit by rotation invariance. On the honeycomb lattice the maximal violation of full rotational symmetry occurs for directions differing by a $\pi/6$ angle, and therefore, taking into account its discrete rotational symmetry, also by a $\pi/2$ angle. So a good test of rotation invariance is provided by the ratio between masses

extracted from the long-distance behaviors of two orthogonal wall-wall correlation functions constructed with $G(x)$, such as μ_v/μ_h.

In the O(N) σ models, in order to evaluate the ratio between the Λ parameters of the $\overline{\text{MS}}$ renormalization scheme and the honeycomb nearest-neighbor lattice regularization. We calculated, in perturbation theory, the correlation function

$$G(x_+ - y_+) = \langle \vec{s}_{x_+} \cdot \vec{s}_{y_+} \rangle. \qquad \text{(B8)}$$

In the x space we obtained [neglecting $O(a^2)$ terms]

$$G(x) = 1 + \frac{N-1}{N} tF(a/x) + O(t^2),$$

$$F(a/x) = \frac{1}{2\pi}\left(\ln\frac{a}{x} - \gamma_E - \ln 2\right). \qquad \text{(B9)}$$

In the p space

$$\widetilde{G}(k) = \frac{N-1}{N}\frac{t}{k^2}\left[1 + \frac{t}{N}\left(D(ak) + \frac{1}{3\sqrt{3}}\right) + O(t^2)\right],$$

$$D(ak) = \frac{1}{2\pi}(\ln ak - 2\ln 2). \qquad \text{(B10)}$$

The relevant formulas required by the above calculations can be found in Ref. [4].

Comparing the above results with the two-point Green's function renormalized in the $\overline{\text{MS}}$ scheme [cf. Eq. (A11)], one can obtain the ratio of Λ parameters:

$$\frac{\Lambda_{\overline{\text{MS}}}}{\Lambda_h} = 4\exp\left(\frac{\pi}{N-2}\frac{2}{3\sqrt{3}}\right) \qquad \text{(B11)}$$

where Λ_h is the Λ parameter of the honeycomb lattice, and also

$$\frac{\Lambda_h}{\Lambda_s} = \sqrt{2}\exp\left[\frac{\pi}{N-2}\left(\frac{1}{2} - \frac{2}{3\sqrt{3}}\right)\right]. \qquad \text{(B12)}$$

We also give a few orders of the perturbative expansion of the internal energy

$$E = 1 - \frac{N-1}{N}\frac{t}{3\sqrt{3}} - \frac{N-1}{N^2}\frac{t^2}{54} + O(t^3). \qquad \text{(B13)}$$

APPENDIX C: COMPLEX-TEMPERATURE SINGULARITIES AT $N=\infty$ ON THE TRIANGULAR AND HONEYCOMB LATTICES

In this appendix we will compute the complex-temperature singularities for the $N=\infty$ model on the various lattices we considered. We will follow closely the analysis of Ref. [7] for the square lattice. The $N=\infty$ solution is written in all cases in terms of a variable w related to the inverse temperature β by the gap equation, which has the generic form

$$\beta = h(w)\rho(w)K(\rho(w)) \equiv b(w) \qquad (C1)$$

for suitable analytic functions $h(w)$ and $\rho(w)$ and variable w, which will be defined below. Here $K(w)$ is the complete elliptic integral of the first kind. In general, $b(w)$ will be defined on the complex plane with suitable cuts. For the purpose of computing the singularities of the inverse function $w(\beta)$ we will be forced to consider $b(w)$ on its Riemann surface $\mathcal{R}$. Moreover, our discussion will be only local and thus we will determine all singularities which appear in the Riemann surface of $w(\beta)$. Notice that not all of them will necessarily appear in the principal sheet of $w(\beta)$.

Let us now consider a point $w_0 \in \mathcal{R}$ and let $\beta_0 = b(w_0)$. To study $w(\beta)$ in the neighborhood of β_0 let us expand $b(w)$ around w_0. If $b'(w_0)$ is different from zero, then $w(\beta)$ is obviously analytic in the neighborhood of β_0 and admits an expansion of the form

$$w = w_0 + \frac{1}{b'(w_0)}(\beta - \beta_0) + O((\beta - \beta_0)^2). \qquad (C2)$$

Instead, if $b'(w_0) = 0$, β_0 is a singular point. Indeed, let k be the smallest integer such that $b^{(k)}(w_0) \neq 0$. Then in the neighborhood of β_0 we have

$$w = w_0 + \left(\frac{k!}{b^{(k)}(w_0)}\right)^{1/k}(\beta - \beta_0)^{1/k} + O((\beta - \beta_0)^{2/k}), \qquad (C3)$$

and therefore β_0 is a kth-root singular point of $w(\beta)$. Thus, in order to determine the singularities of $w(b)$, we must determine the zeros of $b'(w)$ on the Riemann surface of the function $b(w)$.

In addition to the expansion in β we will be interested in expanding our observables in terms of the energy E. We want thus to study the singularities of the various observables when expressed in terms of E. In practice, we must study the functions $w(E)$ and $\beta(E)$.

For all lattices we consider we have

$$E = \frac{\alpha}{\beta} + e(w) = \frac{\alpha}{b(w)} + e(w) \qquad (C4)$$

where α is a constant and $e(w)$ an analytic function. We will verify in each specific case that the zeros of $b(w)$ do not give rise to any singularity. Then by an argument completely analogous to the one given for $w(\beta)$, the singularities of $w(E)$ are determined by the zeros of dE/dw over the Riemann surface of the function $E(w)$, which, because of the fact that $e(w)$ is a simple rational function of w, coincides with the Riemann surface of $b(w)$.

Finally, let us discuss $\beta(E)$. Of course, locally we can rewrite it as $\beta(w(E))$. We shall show that $d\beta/dw$ and dE/dw never vanish at the same point. Then it is simple to convince oneself that the singularities of $\beta(E)$ coincide with those of $w(E)$.

1. Analytic structure of the complete elliptic integral $K(w)$

The analytic properties of the function $K(w)$ are well known (cf., e.g., Refs. [26,27]). First of all, $K(w)$ is really a function of w^2; indeed, it has a representation in terms of hypergeometric functions as [8,27]

$$K(w) = \frac{\pi}{2}\,_2F_1\left(\frac{1}{2},\frac{1}{2};1;w^2\right). \qquad (C5)$$

From this representation one may see that $K(w)$ is analytic in the w^2 plane cut along the real axis from 1 to infinity. We want now to discuss the extension of $K(w)$ to its Riemann surface. First of all, let us introduce the θ function

$$\theta_3(v|\tau) = \sum_{m=-\infty}^{\infty} e^{\pi i(m^2\tau + 2mv)}. \qquad (C6)$$

$\theta_3(v|\tau)$ is an entire function of τ and v for $\mathrm{Im}\,\tau > 0$. Moreover, it satisfies the properties (cf. Ref. [26], Chap. 5)

$$\theta_3(v|\tau+2) = \theta_3(v|\tau), \qquad (C7)$$

$$\theta_3(v/\tau|-1/\tau) = \sqrt{-i\tau}\,e^{\pi i v^2/\tau}\theta_3(v|\tau). \qquad (C8)$$

In terms of $\theta_3(v|\tau)$ we define the modular function

$$\lambda(\tau) = e^{\pi i\tau}\frac{\theta_3^4(-\tau/2|\tau)}{\theta_3^4(0|\tau)} \qquad (C9)$$

which is also an entire function of τ for $\mathrm{Im}\,\tau > 0$. The function $\lambda(\tau)$ has several important properties (cf. Ref. [26], Chap. 7).

(i) Consider the group Γ_2 of transformations

$$\tau' = \frac{a\tau + b}{c\tau + d} \qquad (C10)$$

with

$$M \equiv \begin{pmatrix} a & b \\ c & d \end{pmatrix} \in \mathrm{SL}(2,Z), \quad \begin{pmatrix} a & b \\ c & d \end{pmatrix} \equiv \begin{pmatrix} 1 & 0 \\ 0 & 1 \end{pmatrix} \bmod 2. \qquad (C11)$$

The function $\lambda(\tau)$ is invariant under Γ_2, i.e., $\lambda(\tau) = \lambda(\tau')$. Let us notice that Γ_2 is generated by the transformations

$$\tau' = \tau + 2, \qquad (C12)$$

$$\tau' = \frac{\tau}{2\tau + 1}. \qquad (C13)$$

(ii) Let D be the domain of the complex plane bounded by the lines $\mathrm{Re}\,\tau = \pm 1$ and the circles $|\tau \pm 1/2| = 1/2$, including the boundaries with $\mathrm{Re}\,\tau < 0$. Then for every τ' with $\mathrm{Im}\,\tau' > 0$ there exists a unique $\tau \in D$ and a transformation (C10) connecting τ and τ'. Thus D is the *fundamental domain* of the group Γ_2.

(iii) If c is a complex number different from 0 and 1, the equation $\lambda(\tau) = c$ has one and only one solution in D. Moreover, $\lambda(x + i\infty) = 0$ for real x.

Using the function $\lambda(\tau)$ we obtain a complete parametrization of the Riemann surface of $K(w)$. Indeed, because of

the last property, we can perform the change of variables $w^2 = \lambda(\tau)$, $\tau \in D$; then it can be shown that [27]

$$K(\sqrt{\lambda(\tau)}) = \frac{\pi}{2}\,\theta_3^2(0|\tau). \qquad (C14)$$

The complete Riemann surface is then obtained by letting τ vary in the whole upper complex plane. Notice that since $\theta_3(0|\tau)$ never vanishes for $\mathrm{Im}\,\tau > 0$, the analytic extension of $K(w)$ is always nonzero.

We want now to express the analytic extension of $K(w)$ on every Riemann sheet in terms of functions defined on the principal sheet. This will allow us to go back using w^2 as fundamental variable. This is easily accomplished using the second property of $\lambda(\tau)$. Indeed, if τ' is a generic point with positive imaginary part, there exists a unique $\tau \in D$ such that (C10) holds for suitable integers a, b, c, and d satisfying Eq. (C11). Thus

$$\theta_3^2(0|\tau') = \theta_3^2\!\left(0\left|\frac{a\tau+b}{c\tau+d}\right.\right). \qquad (C15)$$

To compute the right-hand side (RHS), let us notice that the transformations (C10) are generated by Eqs. (C12) and (C13). Then, using Eq. (C7) and

$$\theta_3^2\!\left(0\left|\frac{\tau}{\pm 2\tau+1}\right.\right) = \theta_3^2(0|\tau) \pm 2i\,\theta_3^2(0|-1/\tau), \quad (C16)$$

which can be derived from Eqs. (C7) and (C8), we get easily, by induction,

$$\theta_3^2(0|\tau') = s[d\,\theta_3^2(0|\tau) + ic\,\theta_3^2(0|-1/\tau)], \qquad (C17)$$

where s assumes the values ± 1. The presence of this sign is due to the fact that the matrix in Eq. (C11) which corresponds to the transformation (C10) is defined up to a sign. If we define

$$T_1 \equiv \begin{pmatrix} 1 & 2 \\ 0 & 1 \end{pmatrix}, \quad T_2 \equiv \begin{pmatrix} 1 & 0 \\ 2 & 1 \end{pmatrix}, \qquad (C18)$$

and fix the signs in M so that M is a product of T_1 and T_2 and their inverses only, then $s = 1$. Finally, using $\lambda(-1/\tau) = 1 - \lambda(\tau)$ which easily follows from Eq. (C8), we get

$$\frac{\pi}{2}\,\theta_3^2(0|\tau') = s[dK(w) + icK(\sqrt{1-w^2})] \qquad (C19)$$

with $w^2 = \lambda(\tau')$. As we shall see, the sign s plays no role in the subsequent discussion.

We have thus reached the following result [7]: the Riemann surface of $K(w)$ is obtained by considering matrices M generating transformations belonging to Γ_2: as M is defined modulo a sign we can always assume $d > 0$. Then each sheet of the Riemann surface is labeled by the pair (d,c) of one row. [We write (d,c) instead of (c,d) to use the same notation as in Ref. [7].] The extension $K_{(d,c)}(w)$ on this sheet is given by

$$s[dK(w) + icK(\sqrt{1-w^2})] \qquad (C20)$$

where s is a sign depending on M.

Finally, let us notice that $K(\sqrt{z^*}) = K(\sqrt{z})^*$ so that $K_{(d,c)}(\sqrt{z^*}) = K_{(d,-c)}(\sqrt{z})^*$. This observation will allow us to consider only the case $d,c > 0$.

2. Location of the singularities

The singularities of $w(\beta)$ on the square lattice have been studied in Ref. [7]. Here we will restrict our attention to the case of triangular and honeycomb lattices. Let us first simplify the expressions (42) and (56) by introducing new variables

$$w = \left(1 + \frac{z}{6}\right)^{1/2} \text{ on the triangular lattice,} \qquad (C21)$$

$$w = \left(1 + \frac{z}{4}\right) \text{ on the honeycomb lattice.} \qquad (C22)$$

Then

$$\beta = \frac{1}{2\pi}\,\frac{1}{\sqrt{3w}}\,\rho K(\rho) \text{ on the triangular lattice,} \quad (C23)$$

$$\beta = \frac{1}{2\pi}\,\sqrt{3w}\,\rho K(\rho) \text{ on the honeycomb lattice,} \quad (C24)$$

where, for both lattices,

$$\rho = \frac{4\sqrt{w}}{(3w-1)^{3/2}(w+1)^{1/2}}. \qquad (C25)$$

The gap equation has an important property: as

$$\rho(-w)^2 = \frac{\rho(w)^2}{\rho(w)^2 - 1} \qquad (C26)$$

and the elliptic integral satisfies the property $K(iz/\sqrt{1-z^2}) = \sqrt{1-z^2}K(z)$, we can immediately derive that $\beta(-w) = \pm\beta(w)$ where the upper (lower) sign refers to the triangular (honeycomb) lattice.

Let us now discuss the Riemann surface of $b(w)$. As ρ^2 is a meromorphic function with two poles in the w plane for $w = 1/2$ and $w = -1$, we can apply the discussion of the previous paragraph. We must then consider the prefactor in front, which contains a square root with two branching points and which has thus a double-sheeted Riemann surface. The Riemann surface is then labeled by two integers (d,c) as we discussed in the previous paragraph, and a sign s which specifies the sheet of the Riemann surface of the prefactor. Thus we have

$$\beta_{s,d,c} = s\,\frac{1}{2\pi}\,\frac{1}{\sqrt{3w}}\,\rho K_{(d,c)}(\rho) \text{ on the triangular lattice,}$$
$$\qquad (C27)$$

$$\beta_{s,d,c} = s\,\frac{1}{2\pi}\,\sqrt{3w}\,\rho K_{(d,c)}(\rho) \text{ on the honeycomb lattice.}$$
$$\qquad (C28)$$

TABLE XII. Analysis of the 29th order strong-coupling series of $E^{-1}u(E)$ and $\beta^{-1}u(\beta)$, where $u \equiv m_2^2/(\chi m_4)$, for $N=3$ on the honeycomb lattice. The first two lines report the values of u as obtained from the $[l/m]$ PA's and Dln-PA's at $E=1$. The last two lines report the values of u from $[l/m]$ PA's and Dln-PA's at $\beta=0.85$ corresponding to $\xi \simeq 22$. A pole has been detected at $E_0 = -0.114\,04$, corresponding to $M_G^2 = -16.000$. Asterisks mark defective PA's.

		13/13	13/14	12/15	14/14	13/15	12/16	14/15	13/16	12/17
$E=1$	PA	0.2511	0.2484	0.2498	*	*	*	0.2482	0.2495	0.2526
	DLPA	0.2465	0.2469	0.2485	0.2467	0.2467	*			
$\beta=0.85$	PA	0.2490	0.2490	0.2490	0.2489	0.2482	0.2488	0.2489	0.2490	0.2490
	DLPA	0.2493	0.2494	0.2488	*	*	*			

To identify the singularities we must then find the zeros in the complex plane of

$$\frac{d\beta_{s,d,c}}{dw} = -\frac{s\rho}{4\pi w}\frac{1}{(3w)^{\pm 1/2}}\left[\pm K_{(d,c)}(\rho)\right.$$

$$\left. + E_{(d,c)}(\rho)\frac{(3w-1)^2}{(3w+1)(w-1)}\right], \qquad \text{(C29)}$$

where the upper (lower) sign refers to the triangular (honeycomb) lattice and

$$E_{(d,c)}(w) = dE(w) + ic[K(\sqrt{1-w^2}) - E(\sqrt{1-w^2})]. \qquad \text{(C30)}$$

The zeros of Eq. (C29) have been studied numerically as in Ref. [7]. In Table XIII we report the solutions with positive real and imaginary parts we have found for the lowest values of (d,c). We have verified that in all cases $d^2\beta_{s,d,c}/dw^2 \neq 0$ at the singularity: thus all points are square-root branch points. Notice that if β is a singularity $-\beta$ and $\pm\beta^*$ are also singularities. Our results are somewhat different from those of Ref. [7] on the square lattice. Indeed, in our case we

have found more than one zero with $\text{Re}\beta>0$ and $\text{Im}\beta>0$ on each sheet. The principal sheet is an exception, as it is free of singularity for the triangular lattice, while it contains a pair of purely imaginary singularities for the honeycomb lattice. We stress that our search for zeros of Eq. (C29) has been done numerically and thus we cannot exclude the possibility that some zeros have been overlooked. However, we are confident that at least in the region $|\beta|<2$ our list is exhaustive for the values of (d,c) we have examined.

To check the value of the zero with lowest $|\beta|$ we can compare with a direct determination of the singularity from an analysis of the high-temperature series of χ by Dln-PA's or first order inhomogeneous integral approximants (IA's). In Table XIV we report the results of such an analysis. These numbers are in very good agreement with the exact results, although the spread of the Dln-PA's largely underestimates the true error. This is probably due to the fact that Dln-PA's are unable to reconstruct the exact singularity. Indeed, for $\beta \to \beta_{\text{sing}}$ we have $\chi = \chi_0 + \chi_1(\beta-\beta_{\text{sing}})^{1/2} + \cdots$: as $\chi_0 \neq 0$ this behavior can be reproduced by IA's but not by Dln-PA's.

Let us also notice that for the triangular lattice only the singularities with positive real part appear in our analysis.

TABLE XIII. Singularities in the complex β plane for the triangular and honeycomb lattices at $N=\infty$ with positive real and imaginary parts for the lowest values of (d,c). The singularity on the real axis for the honeycomb lattice ($\beta=0.627\,168$) does not appear on the principal sheet of $w(\beta)$ as the corresponding w-value is $0.962\,998i$.

(d,c)	Triangular	Honeycomb
(1,0)		0.3620955333 i
(1,±2)	0.206711 + 0.181628 i	0.482696 + 0.628020 i
	0.685669 + 0.749077 i	0.449772 + 0.583632 i
		0.627168
(3,±4)	0.240692 + 0.486530 i	0.566020 + 1.476842 i
	0.564118 + 0.203430 i	0.946032 + 1.663513 i
	1.469137 + 2.118380 i	1.237526 + 0.266631 i
(5,±6)	0.260362 + 0.780732 i	0.627495 + 2.353352 i
	0.920774 + 0.210433 i	1.413547 + 2.691806 i
	2.244964 + 3.482094 i	1.836347 + 0.535158 i
(5,±8)	0.662428 + 0.858005 i	1.502252 + 2.655737 i
	0.980284 + 0.576976 i	1.907210 + 2.926524 i
	2.847075 + 3.621622 i	2.022490 + 1.997953 i
		2.500324 + 0.265750 i
(7,±8)	0.274172 + 1.072281 i	0.669817 + 3.225087 i
	1.763190 + 0.911108 i	1.881646 + 3.718975 i
	3.019312 + 4.844833 i	2.432118 + 0.804519 i

TABLE XIV. For $N=\infty$ we report the zeros closest to the origin as obtained by an analysis of the strong-coupling series of χ by Dln-PA's and IA's. We consider the series at 15th and 30th order on the triangular lattice, and 30th and 60th order on the honeycomb lattice. γ_s is the exponent corresponding to the singularity β_s in the IA analysis [20] (its exact value is $\gamma_s=-1/2$). The Dln-PA analysis does not provide stable estimates of γ_s. The values we quote are average and maximum spread of the Dln-PA's [m/n] with $5\leq m\leq 9$ (series with 15 terms), $12\leq m\leq 17$ (30 terms), and $27\leq m\leq 32$ (60 terms); for the IA we use in all cases six quasidiagonal approximants.

Lattice	n	β_s (Dln-PA)	β_s (IA)	γ_s (IA)
Triangular	15	$0.214(4)\pm i0.1838(2)$	$0.206(1)\pm i0.1811(6)$	$0.54(7)\mp i\,0.07(6)$
	30	$0.2084(2)\pm i0.1821(2)$	$0.206712(1)\pm i0.181628(1)$	$-0.4997(4)\mp i\,0.0001(2)$
Honeycomb	30	$\pm i0.3648(8)$	$\pm i0.36211(3)$	$-0.50(2)\mp i\,0.001(6)$
	60	$\pm i0.36270(4)$	$\pm i0.3620955327(5)$	$-0.500001(1)\mp i0.000001(1)$

With series with 30 terms or more it is also possible to get an estimate of a second singularity. For the triangular lattice the series with 30 terms has a second singularity at $\beta=-0.698(6)\pm i0.776(5)$, which corresponds to the second point in the sheet with $d=1$ and $c=2$. For the honeycomb lattice we get $\pm0.449(13)\pm i0.610(17)$ (30 terms) and $\pm0.4504(7)\pm i0.5909(25)$ (60 terms). The IA's are less stable and the 30-term series do not yield any result. With 60 terms on the honeycomb lattice we get $\pm0.449(3)\pm i0.585(2)$, which is in perfect agreement with the exact result.

As well as considering the series in β we have also considered series with the energy E as variable. In this case we must consider the zeros of dE/dw. Explicitly, for the three lattices we have (for the square lattice we take $w=\rho_s$):

$$\frac{dE}{dw}=\frac{1}{4\beta^2}\frac{d\beta}{dw}-\frac{1}{w^2}, \quad \text{square lattice}, \quad \text{(C31)}$$

$$\frac{dE}{dw}=\frac{1}{6\beta^2}\frac{d\beta}{dw}+3w, \quad \text{triangular lattice}, \quad \text{(C32)}$$

$$\frac{dE}{dw}=\frac{1}{3\beta^2}\frac{d\beta}{dw}+1, \quad \text{honeycomb lattice}. \quad \text{(C33)}$$

It is evident from these formulas that $dE/dw\neq0$ where $d\beta/dw=0$. Thus, as we said at the beginning of this appendix, the analysis of dE/dw provides all singularities of $w(E)$ and $\beta(E)$. We get for the nearest singularities:

$$E=\pm0.330\,261\,131\,671i, \quad \text{square lattice},$$

$$E=-0.290\,013\,856\,190$$

$$\pm0.138\,180\,553\,789i, \quad \text{triangular lattice},$$

$$E=\pm0.303\,078\,379\,027$$

$$\pm0.402\,035\,415\,796i, \quad \text{honeycomb lattice}.$$

For the square and honeycomb lattices the singularity appears on the principal sheet of $E(w)$ while for the triangular lattice it belongs to the sheet with $(d,c)=(1,2)$.

From the position of the singularities we can now compute the convergence radius of the high-temperature series on the real axis. In terms of the correlation length, we find that the series converge up to ξ_{conv} where

(1) square lattice: β series, $\xi_{\text{conv}}=3.171\,60$; E series, $\xi_{\text{conv}}=1.384\,03$,

(2) triangular lattice: β series, $\xi_{\text{conv}}=2.989\,25$; E series: $\xi_{\text{conv}}=1.667\,06$,

(3) honeycomb lattice: β series, $\xi_{\text{conv}}=1.000\,02$; E series: $\xi_{\text{conv}}=2.434\,50$.

The series converge thus in a very small β disk: however PA's and IA's are quite successful in providing good estimates in a larger domain of the β plane: indeed, for the square (triangular, honeycomb) lattice, series with 21 (15,30) terms give estimates which differ from the exact result by less than 1% till $\xi\approx10$ (5,15).

3. Conformal transformations

Once the singularities are known one can use a conformal transformation to get rid of the nearest ones (cf., e.g. [9],) and thus accelerate the convergence of the approximants.

Let us first consider the triangular lattice which has two singularities located at $\beta=\rho e^{\pm i\theta}$ with $\rho=0.275\,169\,111\,05$, $\theta=0.720\,896\,055$. As in Ref. [7] we consider a transformation of the form

$$\beta=\rho w[1+P(w)Q(w)+\mu Q(w)^2] \quad \text{(C34)}$$

where $Q(w)=1-2w\cos\theta+w^2$ is a polynomial which vanishes for $w=e^{\pm i\theta}$. $P(w)$ is determined by requiring that $d\beta/dw=0$ for $w=e^{\pm i\theta}$. The simplest polynomial with this property is given by

$$P(w)=-\frac{1}{2\sin^2\theta}(\cos2\theta-w\cos\theta). \quad \text{(C35)}$$

We will also consider a second possibility given by

$$\beta=\rho w\left[1-\frac{1}{4}\left(\frac{\cos4\theta}{\sin^2 2\theta}-\frac{\cot2\theta}{\sin2\theta}w^2\right)(1-2w^2\cos2\theta+w^4)\right.$$

$$\left.+\mu(1-2w^2\cos2\theta+w^4)^2\right]. \quad \text{(C36)}$$

This transformation would also work if we had four singularities at $\beta=\pm\rho e^{\pm i\theta}$. It is easy to see that for $\theta=\pi/4$ it reduces to the transformation used in [7] for the square lat-

tice. For the honeycomb lattice the nearest singularities are $\beta = \pm i\rho$ with $\rho = 0.362\,095\,533\,3$. We can thus use Eq. (C34) with $\theta = \pi/2$: i.e.,

$$\beta = \rho w \left[1 + \frac{1}{2}(1+w^2) + \mu(1+w^2)^2 \right]. \qquad \text{(C37)}$$

In all cases μ is a free parameter which can be used to optimize the transformation.

In order to compare the series with and without conformal transformation we have compared the results for the magnetic susceptibility for series with 15 and 30 terms on the triangular lattice and honeycomb lattice, respectively.

For the triangular lattice we have considered the [6/7], [7/6], [6/8], [7/7], and [8/6] Dln-PA's. For the series without conformal transformation we have found that all PA's have singularities on the real axis or with a small imaginary part (Im$\beta \lesssim 0.2$) with $0.4 \lesssim \text{Re}\beta \lesssim 0.6$. Excluding only the PA with the nearest singularity ([6/7] for which $\beta_{\text{sing}} \simeq 0.414$), we find that the estimates agree within 1% till $\beta \approx 0.33$ ($\xi = 5.31$) where we get $\chi = 57.69(56)$ (this value is the average of the estimates of the various PA's, while the error is the maximum difference between two different PA's), which must be compared with the exact value $\chi = 56.9837$. Let us now consider the series obtained from the conformal transformation (C34). The results are now much more stable: at $\beta = 0.33$ the series with $\mu = 0$ gives $\chi = 56.978(25)$ while for $\mu = 0.5$ we get $\chi = 56.9804(24)$. The estimates of the series with $\mu = 0$ agree within 1% till $\beta = 0.46$ ($\xi = 21.58$), where we get $\chi = 672(6)$ (exact value $\chi = 674.86$), while for the case $\mu = 0.5$ the same is true till $\beta = 0.61$ ($\xi = 110.27$). In this last case, however, the fluctuations of the approximants are not a good estimate of the error: indeed, we get $\chi = 12\,861(126)$ to be compared with the exact value $\chi = 13\,290$. The estimates agree within 1% with the exact result only till $\beta = 0.56$ ($\xi = 64.00$).

Let us now consider the second transformation. The Dln-PA's for $\mu = 0$ do not have any singularity on the real axis for $\beta < 3$ and their estimates are extremely stable. For the value we have considered before, $\beta = 0.33$, they give $\chi = 56.9808(5)$, which is in excellent agreement with the exact value although the error bar is clearly underestimated. The five different PA's agree within 1% till $\beta = 0.72$ ($\xi = 365.05$), where the estimate is $\chi = 110\,200(1100)$ to be compared with the exact value $\chi = 123\,387$. Again, the error bar is underestimated and the true error is 11%. Indeed, the estimate from the PA's agrees with the exact value within 1% only till $\beta = 0.53$ ($\xi = 46.18$).

If we use the series with $\mu \neq 0$ the stability of the PA's decreases and singularities on the real axis begin to appear near the origin. For $\mu = 0.1$, the PA's are still reasonably stable and we get, for $\beta = 0.33$, $\chi = 57.03(6)$. The PA's agree within 1% till $\beta = 0.41$ ($\xi = 12.55$), where we get $\chi = 257.9(2.4)$, to be compared with the estimate with $\mu = 0$, $\chi = 255.83(2)$, and the exact value $\chi = 256.02$.

An analogous analysis can be done for the honeycomb lattice. In this case we have considered the [14/14], [13/16], [14/15], [15/14], and [16/13] Dln-PA's, excluding in each case those having a singularity on the positive real axis with $\beta < 3$. We find that PA's of the standard series agree within 1% till $\beta = 1.15$ ($\xi = 16.23$), where $\chi = 303.2(2.8)$ to be compared with the exact result $\chi = 305.53$. The conformally transformed PA's give instead $\chi = 305.14(69)$ for $\mu = 0$ and $\chi = 305.84(63)$ for $\mu = 0.3$. The conformally transformed PA's agree within 1% till $\beta = 1.35$ ($\xi = 33.50$), where we get $\chi = 1100(15)$ for $\mu = 0$ and $1114(12)$ for $\mu = 0.3$. This should be compared with the exact value $\chi = 1108.13$ and with the estimate from the standard series $\chi = 1073(47)$.

From this analysis it emerges that the conformal transformation is extremely useful, especially for the triangular lattice, where one gets results which are better by a factor of 10–100. Of course, the interesting problem would be to generalize the method to finite values of N. There are two problems here. First of all, the exact location of the singularities is not known. Moreover the exact nature of the singularity must also be determined from the series. The first problem is probably not a very serious one: indeed if we redo the analysis we have presented using the values of the zeros obtained from a Dln-PA analysis of the series itself, the results are essentially unchanged. The really serious problem (at least for low values of N) is the nature of the singularity: indeed, the transformations we have considered apply only to square-root branch points. If the singularity is different new transformations must be used.

APPENDIX D: STRONG-COUPLING SERIES ON THE SQUARE LATTICE

A complete presentation of our strong-coupling series is beyond the scope of the present paper. A forthcoming publication will include all the relevant "raw" series. In order to enable the interested readers to perform their own analysis, we present here just the series for the internal energy E, the magnetic susceptibility χ, the three mass scales M_G^2, M_s^2, and M_d^2, and the renormalization-group-invariant quantity u, on the square lattice, for the most interesting values of N, i.e., $N = 3,4,8$. The following appendixes will be devoted to the triangular and honeycomb lattice.

1. $N=3$

$$E = \beta + \frac{7}{5}\beta^3 - \frac{24}{35}\beta^5 - \frac{3439}{875}\beta^7 - \frac{21872}{1925}\beta^9 - \frac{2876163636}{153278125}\beta^{11} + \frac{236181936}{21896875}\beta^{13} + \frac{9960909191551}{65143203125}\beta^{15} + \frac{2128364407641312}{4665255546875}\beta^{17}$$

$$+ \frac{34746325087320066964}{36692234876171875}\beta^{19} + \frac{42007349682504569392}{548000091048828125}\beta^{21} + O(\beta^{23}), \qquad \text{(D1a)}$$

$$\chi = 1 + 4\beta + 12\beta^2 + \frac{168}{5}\beta^3 + \frac{428}{5}\beta^4 + \frac{1448}{7}\beta^5 + \frac{84144}{175}\beta^6 + \frac{942864}{875}\beta^7 + \frac{2055588}{875}\beta^8 + \frac{6845144}{1375}\beta^9 + \frac{3478216992}{336875}\beta^{10} + \frac{643017322016}{30655625}\beta^{11}$$
$$+ \frac{915294455744}{21896875}\beta^{12} + \frac{125506127121 28}{153278125}\beta^{13} + \frac{120892276630256}{766390625}\beta^{14} + \frac{3896992088570128}{13028640625}\beta^{15} + \frac{50948877169965252}{91200484375}\beta^{16} + \frac{5670666438003413208}{5513483828125}\beta^{17}$$
$$+ \frac{6224368647227625667744}{3335657716015625}\beta^{18} + \frac{6125800535183894564557 44}{183461174380859375}\beta^{19} + \frac{1080648046932437417271696}{183461174380859375}\beta^{20} + \frac{4321920010959667155 8015312}{4219607010759765625}\beta^{21} + O(\beta^{22}),$$
$$(\text{D1b})$$

$$M_G^2 = \beta^{-1} - 4 + \frac{18}{5}\beta + \frac{638}{175}\beta^3 - \frac{32}{25}\beta^4 - \frac{212}{875}\beta^5 - \frac{8256}{875}\beta^6 + \frac{2392562}{336875}\beta^7 - \frac{893248}{30625}\beta^8 + \frac{67614504}{13934375}\beta^9 + \frac{1315441408}{11790625}\beta^{10} - \frac{305969023608}{766390625}\beta^{11}$$
$$+ \frac{515730116144}{766390625}\beta^{12} - \frac{129453356216124}{456002421875}\beta^{13} - \frac{38248494356608}{26823671875}\beta^{14} + \frac{15923896875925326898}{3335657716015625}\beta^{15} - \frac{1027275161540 55776}{25080133203125}\beta^{16}$$
$$- \frac{11977717369812123408}{1467689395046875}\beta^{17} + \frac{8720095096679140 65856}{26208739197265625}\beta^{18} - \frac{12129265223066172243071804}{274274455699384765625}\beta^{19} + O(\beta^{20}),$$
$$(\text{D1c})$$

$$M_s^2 = \beta^{-1} - 4 + \frac{18}{5}\beta + \frac{638}{175}\beta^3 - \frac{32}{25}\beta^4 - \frac{772}{875}\beta^5 - \frac{912}{175}\beta^6 - \frac{1730018}{336875}\beta^7 - \frac{790736}{153125}\beta^8 - \frac{226737372}{13934375}\beta^9 + \frac{1892118016}{58953125}\beta^{10} - \frac{280950072668}{3831953125}\beta^{11}$$
$$+ \frac{642095551792}{3831953125}\beta^{12} - \frac{451334756421336}{2280012109375}\beta^{13} + \frac{1890027233038144}{4694142578125}\beta^{14} - \frac{269818891521799734}{1282945275390625}\beta^{15} + O(\beta^{16}),$$
$$(\text{D1d})$$

$$M_d^2 = \beta^{-1} - 4 + \frac{18}{5}\beta + \frac{122}{35}\beta^3 - \frac{4086}{875}\beta^5 - \frac{16737807}{1684375}\beta^7 - \frac{18994322761}{1532781250}\beta^9 + \frac{21507562283}{3831953125}\beta^{11} + \frac{7336555515481743}{79800423828125}\beta^{13} + O(\beta^{15}), \quad (\text{D1e})$$

$$u = 4\beta - 48\beta^2 + \frac{2808}{5}\beta^3 - \frac{32832}{5}\beta^4 + \frac{2686616}{35}\beta^5 - \frac{157029504}{175}\beta^6 + \frac{9178202064}{875}\beta^7 - \frac{107291190016}{875}\beta^8 + \frac{13796318675224}{9625}\beta^9 - \frac{5644659282845824}{336875}\beta^{10}$$
$$+ \frac{30023104630997669536}{153278125}\beta^{11} - \frac{31905781361056472448}{13934375}\beta^{12} + \frac{315591420176616436544}{11790625}\beta^{13} - \frac{2397977006665 26161503744}{766390625}\beta^{14}$$
$$+ \frac{238270573588813562802881872}{65143203125}\beta^{15} - \frac{19497320035839102967394487936}{456002421875}\beta^{16} + \frac{3331130440560593125866977 67112}{666465078125}\beta^{17}$$
$$- \frac{19489567025124572887718011335312384}{3335657716015625}\beta^{18} + \frac{2506117021969764882798368740582197376}{36692234876171875}\beta^{19} - \frac{1464798277996645191453539504 07208628096}{183461174380859375}\beta^{20}$$
$$+ \frac{3938330210240271860257180702284734986 4016}{4219607010759765625}\beta^{21} + O(\beta^{22}).$$
$$(\text{D1f})$$

2. $N=4$

$$E = \beta + \frac{4}{3}\beta^3 - \frac{4}{3}\beta^5 - \frac{28}{5}\beta^7 - \frac{472}{45}\beta^9 - \frac{344}{945}\beta^{11} + \frac{256324}{2835}\beta^{13} + \frac{12150256}{42525}\beta^{15} + \frac{18845248}{91125}\beta^{17} - \frac{68510312996}{63149625}\beta^{19} - \frac{3399769545 32}{63149625}\beta^{21} + O(\beta^{23}),$$
$$(\text{D2a})$$

$$\chi = 1 + 4\beta + 12\beta^2 + \frac{100}{3}\beta^3 + 84\beta^4 + \frac{596}{3}\beta^5 + \frac{1348}{3}\beta^6 + \frac{14564}{15}\beta^7 + \frac{91132}{45}\beta^8 + \frac{549332}{135}\beta^9 + \frac{213868}{27}\beta^{10} + \frac{8483180}{567}\beta^{11} + \frac{77643788}{2835}\beta^{12}$$
$$+ \frac{138079108}{2835}\beta^{13} + \frac{3569641036}{42525}\beta^{14} + \frac{17867938876}{127575}\beta^{15} + \frac{1066237156}{4725}\beta^{16} + \frac{74408983028}{212625}\beta^{17} + \frac{992250411932}{1913625}\beta^{18} + \frac{45911479386812}{63149625}\beta^{19}$$
$$+ \frac{11971698881708}{12629925}\beta^{20} + \frac{69463206903148}{63149625}\beta^{21} + O(\beta^{22}),$$
$$(\text{D2b})$$

$$M_G^2 = \beta^{-1} - 4 + \frac{11}{3}\beta + \frac{34}{9}\beta^3 - \frac{4}{3}\beta^4 - \frac{224}{135}\beta^5 - \frac{80}{9}\beta^6 + \frac{4}{81}\beta^7 - \frac{544}{45}\beta^8 - \frac{58150}{1701}\beta^9 + \frac{75032}{405}\beta^{10} - \frac{7465004}{18225}\beta^{11} + \frac{20575936}{42525}\beta^{12} + \frac{204232808}{382725}\beta^{13}$$
$$- \frac{359904856}{127575}\beta^{14} + \frac{34575314246}{5740875}\beta^{15} - \frac{938720152}{382725}\beta^{16} - \frac{3116875126738}{189448875}\beta^{17} + \frac{47791394648}{1148175}\beta^{18} - \frac{128064328183586}{3978426375}\beta^{19} + O(\beta^{20}),$$
$$(\text{D2c})$$

$$M_s^2 = \beta^{-1} - 4 + \frac{11}{3}\beta + \frac{34}{9}\beta^3 - \frac{4}{3}\beta^4 - \frac{314}{135}\beta^5 - \frac{14}{3}\beta^6 - \frac{836}{81}\beta^7 + \frac{404}{405}\beta^8 - \frac{215318}{8505}\beta^9 + \frac{4700}{81}\beta^{10} - \frac{443038}{6075}\beta^{11} + \frac{24410738}{127575}\beta^{12} - \frac{24732128}{382725}\beta^{13}$$
$$+ \frac{139715614}{1148175}\beta^{14} + \frac{3172203256}{5740875}\beta^{15} + O(\beta^{16}),$$
$$(\text{D2d})$$

$$M_d^2 = \beta^{-1} - 4 + \frac{11}{3}\beta + \frac{65}{18}\beta^3 - \frac{3341}{540}\beta^5 - \frac{6781}{540}\beta^7 - \frac{1026007}{136080}\beta^9 + \frac{76323223}{2041200}\beta^{11} + \frac{6716460083}{36741600}\beta^{13} + O(\beta^{15}), \quad (\text{D2e})$$

$$u = 4\beta - 48\beta^2 + \frac{1684}{3}\beta^3 - 6560\beta^4 + \frac{229940}{3}\beta^5 - \frac{2686576}{3}\beta^6 + \frac{52315868}{5}\beta^7 - \frac{1833750976}{15}\beta^8 + \frac{192827317268}{135}\beta^9 - \frac{2252963987728}{135}\beta^{10}$$
$$+ \frac{61420977655724}{315}\beta^{11} - \frac{2152899064881952}{945}\beta^{12} + \frac{3593447617956212}{135}\beta^{13} - \frac{1469484644425188368}{4725}\beta^{14} + \frac{7358240125587547636}{2025}\beta^{15}$$
$$- \frac{1805422873668489252736}{42525}\beta^{16} + \frac{31641414417552707 5263484}{637875}\beta^{17} - \frac{1109079895846189652351 4928}{1913625}\beta^{18} + \frac{4751382051424481338 81786892}{7016625}\beta^{19}$$
$$- \frac{4996295906224666012396341020 8}{63149625}\beta^{20} + \frac{58375933833290010617295394 3052}{63149625}\beta^{21} + O(\beta^{22}).$$
$$(\text{D2f})$$

3. $N=8$

$$E = \beta + \frac{6}{5}\beta^3 - \frac{38}{15}\beta^5 - \frac{19924}{2625}\beta^7 + \frac{908}{525}\beta^9 + \frac{103032376}{1771875}\beta^{11} + \frac{284005868}{1771875}\beta^{13} - \frac{801343307824}{3410859375}\beta^{15} - \frac{74654425999556}{30697734375}\beta^{17} - \frac{5113078463377748}{19995352734375}\beta^{19}$$
$$+ \frac{1298678765126787388}{69837345703125}\beta^{21} + O(\beta^{22}),$$
$$(\text{D3a})$$

$$\chi = 1 + 4\beta + 12\beta^2 + \frac{164}{5}\beta^3 + \frac{404}{5}\beta^4 + \frac{548}{3}\beta^5 + \frac{9708}{25}\beta^6 + \frac{2023244}{2625}\beta^7 + \frac{1258836}{875}\beta^8 + \frac{6597628}{2625}\beta^9 + \frac{160511644}{39375}\beta^{10} + \frac{433554844}{70875}\beta^{11}$$

$$+ \frac{4869604484}{590625}\beta^{12} + \frac{17075166692}{1771875}\beta^{13} + \frac{180200884868}{20671875}\beta^{14} + \frac{407707485308}{136434375}\beta^{15} - \frac{18904178053196}{2046515625}\beta^{16} - \frac{861976694991428}{30697734375}\beta^{17} - \frac{2351633289032404}{51162890625}\beta^{18}$$

$$- \frac{421417265877650188}{9976763671875}\beta^{19} + O(\beta^{20}), \tag{D3b}$$

$$M_G^2 = \beta^{-1} - 4 + \frac{19}{5}\beta + \frac{298}{75}\beta^3 + \frac{28}{25}\beta^4 - \frac{5254}{875}\beta^5 - \frac{2128}{375}\beta^6 - \frac{654656}{375}\beta^7 + \frac{98032}{5625}\beta^8 - \frac{95888554}{1771875}\beta^9 + \frac{5421752}{28125}\beta^{10} - \frac{1465956704}{20671875}\beta^{11}$$

$$- \frac{2887857152}{8859375}\beta^{12} + \frac{21729605024744}{10232578125}\beta^{13} - \frac{3782033297144}{930234375}\beta^{14} + \frac{354224260413706}{153488671875}\beta^{15} + \frac{72788687225944}{7308984375}\beta^{16} - \frac{204193924410409426}{4655823046875}\beta^{17}$$

$$+ \frac{40434518800599992}{767443359375}\beta^{18} + \frac{7755263425304938826}{241744658203125}\beta^{19} + O(\beta^{20}), \tag{D3c}$$

$$M_s^2 = \beta^{-1} - 4 + \frac{19}{5}\beta + \frac{298}{75}\beta^3 - \frac{28}{25}\beta^4 - \frac{5744}{875}\beta^5 - \frac{182}{75}\beta^6 - \frac{853316}{39375}\beta^7 + \frac{343772}{28125}\beta^8 - \frac{25597438}{1771875}\beta^9 + \frac{10063732}{140625}\beta^{10} + \frac{7958412578}{103359375}\beta^{11}$$

$$+ \frac{637810442}{44296875}\beta^{12} + \frac{24367739089468}{51162890625}\beta^{13} - \frac{22983973787546}{23255859375}\beta^{14} + \frac{828277050985928}{767443359375}\beta^{15} + O(\beta^{16}), \tag{D3d}$$

$$M_d^2 = \beta^{-1} - 4 + \frac{19}{5}\beta + \frac{23}{6}\beta^3 - \frac{101219}{10500}\beta^5 - \frac{1598337}{87500}\beta^7 + \frac{3042153439}{141750000}\beta^9 + \frac{716944244341}{4961250000}\beta^{11} + \frac{668912806018181}{2728687500000}\beta^{13} + O(\beta^{15}), \tag{D3e}$$

$$u = 4\beta - 48\beta^2 + \frac{2804}{5}\beta^3 - \frac{32736}{5}\beta^4 + \frac{1146292}{15}\beta^5 - \frac{22299088}{25}\beta^6 + \frac{27328827644}{2625}\beta^7 - \frac{106327225472}{875}\beta^8 + \frac{1241049893108}{875}\beta^9 - \frac{72427584678352}{4375}\beta^{10}$$

$$+ \frac{48910909763139412}{253125}\beta^{11} - \frac{190295816674721312}{84375}\beta^{12} + \frac{46643731943589538628}{1771875}\beta^{13} - \frac{2117208265068678482704}{6890625}\beta^{14} + \frac{8321396192774133\,6432836}{23203125}\beta^{15}$$

$$- \frac{1427770122064083058341150\,08}{3410859375}\beta^{16} + \frac{14998421484199502791600778428}{30697734375}\beta^{17} - \frac{2917689406165901738200509\,93776}{51162890625}\beta^{18}$$

$$+ \frac{1328153956920099509461959475\,16884}{1995352734375}\beta^{19} - \frac{86123301574222140902121637239\,4912}{1108529296875}\beta^{20} + \frac{2110982922861147523984004917879\,24004}{23279115234375}\beta^{21} + O(\beta^{22}). \tag{D3f}$$

APPENDIX E: STRONG-COUPLING SERIES ON THE TRIANGULAR LATTICE

We present here the series for the internal energy E, the magnetic susceptibility χ, the two mass scales M_G^2 and M_t^2, and the renormalization-group-invariant quantity u, on the triangular lattice, for $N = 3,4,8$.

1. $N=3$

$$E = \beta + 2\beta^2 + \frac{17}{5}\beta^3 + 4\beta^4 + \frac{132}{175}\beta^5 - \frac{352}{25}\beta^6 - \frac{53833}{875}\beta^7 - \frac{246072}{1225}\beta^8 - \frac{38879794}{67375}\beta^9 - \frac{6397316}{4375}\beta^{10} - \frac{8815166536}{2786875}\beta^{11} - \frac{63896967072}{11790625}\beta^{12}$$

$$- \frac{81729013664}{15640625}\beta^{13} + \frac{23710274924992}{2360483125}\beta^{14} + \frac{4152437111665485\,33}{5016026640625}\beta^{15} + O(\beta^{16}), \tag{E1a}$$

$$\chi = 1 + 6\beta + 30\beta^2 + \frac{672}{5}\beta^3 + \frac{2802}{5}\beta^4 + \frac{388452}{175}\beta^5 + \frac{1478784}{175}\beta^6 + \frac{3891432}{125}\beta^7 + \frac{683113506}{6125}\beta^8 + \frac{131380789212}{336875}\beta^9 + \frac{449739783516}{336875}\beta^{10}$$

$$+ \frac{12494938177056}{2786875}\beta^{11} + \frac{90716274919896}{6131125}\beta^{12} + \frac{368205971277391\,44}{766390625}\beta^{13} + \frac{9067857431725940688}{59012078125}\beta^{14} + \frac{2430225926454897621936}{5016026640625}\beta^{15} + O(\beta^{16}), \tag{E1b}$$

$$M_G^2 = \frac{2}{3}\beta^{-1} - 4 + \frac{56}{15}\beta + \frac{32}{5}\beta^2 + \frac{4552}{525}\beta^3 + \frac{2176}{525}\beta^4 - \frac{40312}{2625}\beta^5 - \frac{288944}{3675}\beta^6 - \frac{13545688}{67375}\beta^7 - \frac{372621008}{1010625}\beta^8 - \frac{338341556368}{459834375}\beta^9 - \frac{33053110624}{18393375}\beta^{10}$$

$$- \frac{5766016722184}{2299171875}\beta^{11} + \frac{279009107673392}{59012078125}\beta^{12} + \frac{72472337922926768}{2149725703125}\beta^{13} + O(\beta^{14}), \tag{E1c}$$

$$M_t^2 = \frac{2}{3}\beta^{-1} - 4 + \frac{56}{15}\beta + \frac{32}{5}\beta^2 + \frac{4496}{525}\beta^3 + \frac{11944}{2625}\beta^4 - \frac{13836}{875}\beta^5 - \frac{6627032}{91875}\beta^6 - \frac{337042602}{1684375}\beta^7 - \frac{1079483686}{2358125}\beta^8 - \frac{408531412013}{459834375}\beta^9$$

$$- \frac{3031149364472}{2299171875}\beta^{10} + O(\beta^{11}), \tag{E1d}$$

$$u = 6\beta - 108\beta^2 + \frac{9552}{5}\beta^3 - 33840\beta^4 + \frac{104891592}{175}\beta^5 - \frac{371571936}{35}\beta^6 + \frac{164533949256}{875}\beta^7 - \frac{20399809562064}{6125}\beta^8 + \frac{2838986498807112}{48125}\beta^9$$

$$- \frac{50284702987803792}{48125}\beta^{10} + \frac{405247036983420442416}{21896875}\beta^{11} - \frac{50244722315696297988096}{153278125}\beta^{12} + \frac{444972341414657282512936\,8}{766390625}\beta^{13}$$

$$- \frac{8669584109460025583796254\,88}{8430296875}\beta^{14} + \frac{182733338163613598761919932\,2672}{1003205328125}\beta^{15} + O(\beta^{16}). \tag{E1e}$$

2. $N=4$

$$E = \beta + 2\beta^2 + \frac{10}{3}\beta^3 + \frac{10}{3}\beta^4 - \frac{8}{3}\beta^5 - \frac{238}{9}\beta^6 - \frac{4312}{45}\beta^7 - \frac{12316}{45}\beta^8 - \frac{30212}{45}\beta^9 - \frac{60434}{45}\beta^{10} - \frac{1579292}{945}\beta^{11} + \frac{24363404}{14175}\beta^{12} + \frac{869521126}{42525}\beta^{13}$$

$$+ \frac{3674593642}{42525}\beta^{14} + \frac{34840110848}{127575}\beta^{15} + O(\beta^{16}), \tag{E2a}$$

$$\chi = 1 + 6\beta + 30\beta^2 + 134\beta^3 + 554\beta^4 + 2162\beta^5 + \frac{24166}{3}\beta^6 + \frac{144242}{5}\beta^7 + \frac{1496254}{15}\beta^8 + \frac{15035566}{45}\beta^9 + \frac{3260594}{3}\beta^{10} + \frac{361103026}{105}\beta^{11}$$

$$+ \frac{50064022798}{4725}\beta^{12} + \frac{450734165906}{14175}\beta^{13} + \frac{439170936682}{4725}\beta^{14} + \frac{11246618825102}{42525}\beta^{15} + O(\beta^{16}), \tag{E2b}$$

$$M_G^2 = \tfrac{2}{3}\beta^{-1} - 4 + \tfrac{34}{9}\beta + \tfrac{20}{3}\beta^2 + \tfrac{248}{27}\beta^3 + \tfrac{32}{9}\beta^4 - \tfrac{9268}{405}\beta^5 - \tfrac{14024}{135}\beta^6 - \tfrac{323204}{1215}\beta^7 - \tfrac{198104}{405}\beta^8 - \tfrac{19703848}{25515}\beta^9 - \tfrac{45897388}{42525}\beta^{10} + \tfrac{357801536}{382725}\beta^{11}$$
$$+ \tfrac{2167022524}{127575}\beta^{12} + \tfrac{83057677936}{1148175}\beta^{13} + O(\beta^{14}),$$
$$\text{(E2c)}$$

$$M_t^2 = \tfrac{2}{3}\beta^{-1} - 4 + \tfrac{34}{9}\beta + \tfrac{20}{3}\beta^2 + \tfrac{245}{27}\beta^3 + \tfrac{107}{27}\beta^4 - \tfrac{18581}{810}\beta^5 - \tfrac{40037}{405}\beta^6 - \tfrac{324218}{1215}\beta^7 - \tfrac{2772953}{4860}\beta^8 - \tfrac{189804947}{204120}\beta^9 - \tfrac{493593379}{765450}\beta^{10} + O(\beta^{11}),$$
$$\text{(E2d)}$$

$$u = 6\beta - 108\beta^2 + 1910\beta^3 - 33828\beta^4 + 599078\beta^5 - 10609380\beta^6 + \tfrac{2818307806}{15}\beta^7 - \tfrac{49910910532}{15}\beta^8 + \tfrac{2651696611738}{45}\beta^9$$
$$- \tfrac{46960305901996}{45}\beta^{10} + \tfrac{17464545810431714}{945}\beta^{11} - \tfrac{220920665969769296}{675}\beta^{12} + \tfrac{82160433528738212702}{14175}\beta^{13} - \tfrac{145502282416479263 4328}{14175}\beta^{14}$$
$$+ \tfrac{5153554644036578704006}{2835}\beta^{15} + O(\beta^{16}).$$
$$\text{(E2e)}$$

3. $N=8$

$$E = \beta + 2\beta^2 + \tfrac{10}{3}\beta^3 + \tfrac{10}{3}\beta^4 - \tfrac{8}{3}\beta^5 - \tfrac{238}{9}\beta^6 - \tfrac{4312}{45}\beta^7 - \tfrac{12316}{45}\beta^8 - \tfrac{30212}{45}\beta^9 - \tfrac{60434}{45}\beta^{10} - \tfrac{1579292}{945}\beta^{11} + \tfrac{24363404}{14175}\beta^{12} + \tfrac{869521126}{42525}\beta^{13}$$
$$+ \tfrac{3674593642}{42525}\beta^{14} + \tfrac{34840110848}{127575}\beta^{15} + O(\beta^{16}),$$
$$\text{(E3a)}$$

$$\chi = 1 + 6\beta + 30\beta^2 + 134\beta^3 + 554\beta^4 + 2162\beta^5 + \tfrac{24166}{3}\beta^6 + \tfrac{144242}{5}\beta^7 + \tfrac{1496254}{15}\beta^8 + \tfrac{15035566}{45}\beta^9 + \tfrac{3260594}{3}\beta^{10} + \tfrac{361103026}{105}\beta^{11}$$
$$+ \tfrac{50064022798}{4725}\beta^{12} + \tfrac{450734165906}{14175}\beta^{13} + \tfrac{439170936682}{4725}\beta^{14} + \tfrac{11246618825102}{42525}\beta^{15} + O(\beta^{16}),$$
$$\text{(E3b)}$$

$$M_G^2 = \tfrac{2}{3}\beta^{-1} - 4 + \tfrac{34}{9}\beta + \tfrac{20}{3}\beta^2 + \tfrac{248}{27}\beta^3 + \tfrac{32}{9}\beta^4 - \tfrac{9268}{405}\beta^5 - \tfrac{14024}{135}\beta^6 - \tfrac{323204}{1215}\beta^7 - \tfrac{198104}{405}\beta^8 - \tfrac{19703848}{25515}\beta^9 - \tfrac{45897388}{42525}\beta^{10} + \tfrac{357801536}{382725}\beta^{11}$$
$$+ \tfrac{2167022524}{127575}\beta^{12} + \tfrac{83057677936}{1148175}\beta^{13} + O(\beta^{14}),$$
$$\text{(E3c)}$$

$$M_t^2 = \tfrac{2}{3}\beta^{-1} - 4 + \tfrac{34}{9}\beta + \tfrac{20}{3}\beta^2 + \tfrac{245}{27}\beta^3 + \tfrac{107}{27}\beta^4 - \tfrac{18581}{810}\beta^5 - \tfrac{40037}{405}\beta^6 - \tfrac{324218}{1215}\beta^7 - \tfrac{2772953}{4860}\beta^8 - \tfrac{189804947}{204120}\beta^9 - \tfrac{493593379}{765450}\beta^{10} + O(\beta^{11}),$$
$$\text{(E3d)}$$

$$u = 6\beta - 108\beta^2 + 1910\beta^3 - 33828\beta^4 + 599078\beta^5 - 10609380\beta^6 + \tfrac{2818307806}{15}\beta^7 - \tfrac{49910910532}{15}\beta^8 + \tfrac{2651696611738}{45}\beta^9$$
$$- \tfrac{46960305901996}{45}\beta^{10} + \tfrac{17464545810431714}{945}\beta^{11} - \tfrac{220920665969769296}{675}\beta^{12} + \tfrac{82160433528738212702}{14175}\beta^{13} - \tfrac{1455022824164792634328}{14175}\beta^{14}$$
$$+ \tfrac{5153554644036578704006}{2835}\beta^{15} + O(\beta^{16}).$$
$$\text{(E3e)}$$

APPENDIX F: STRONG-COUPLING SERIES ON THE HONEYCOMB LATTICE

We present here the series for the internal energy E, the magnetic susceptibility χ, the three mass scales M_G^2, M_v^2, and M_h^2, and the renormalization-group-invariant quantity u, on the honeycomb lattice, for $N = 3,4,8$.

1. $N=3$

$$E = \beta - \tfrac{3}{5}\beta^3 + \tfrac{88}{35}\beta^5 - \tfrac{1761}{175}\beta^7 + \tfrac{14902}{385}\beta^9 - \tfrac{3439769596}{21896875}\beta^{11} + \tfrac{2045078768}{3128125}\beta^{13} - \tfrac{5158924941321}{1861234375}\beta^{15} + \tfrac{28899507590512836}{2425932884375}\beta^{17}$$
$$- \tfrac{172552140904013898254}{3335657716015625}\beta^{19} + \tfrac{415753493847105514488}{1835409748046875}\beta^{21} - \tfrac{8715968136265162257048 57972}{872691449952587890625}\beta^{23} + \tfrac{2973232103934985864357 93176}{67130111534814453125}\beta^{25}$$
$$- \tfrac{938969460961059350452564 48288}{4757152640718994140625}\beta^{27} + \tfrac{6327983006511909061486897651308648928}{716345577406726243832324 21875}\beta^{29} + O(\beta^{31}),$$
$$\text{(F1a)}$$

$$\chi = 1 + 3\beta + 6\beta^2 + \tfrac{51}{5}\beta^3 + \tfrac{84}{5}\beta^4 + \tfrac{978}{35}\beta^5 + \tfrac{7128}{175}\beta^6 + \tfrac{345}{7}\beta^7 + \tfrac{12018}{175}\beta^8 + \tfrac{239238}{1925}\beta^9 + \tfrac{52831068}{336875}\beta^{10} + \tfrac{1370148342}{21896875}\beta^{11} + \tfrac{36519432}{398125}\beta^{12}$$
$$+ \tfrac{2120228676}{3128125}\beta^{13} + \tfrac{81696113448}{109484375}\beta^{14} - \tfrac{4005762392397}{2605728125}\beta^{15} - \tfrac{5554706676084}{3648019375}\beta^{16} + \tfrac{5222504070431 93142}{60648322109375}\beta^{17} + \tfrac{28557036836995675104}{3335657716015625}\beta^{18}$$
$$- \tfrac{84308531983195740042}{2382612654296875}\beta^{19} - \tfrac{5683417110703354254 48}{16678288580078125}\beta^{20} + \tfrac{6099722297292932770 7388}{383600637341796875}\beta^{21} + \tfrac{2621398456210907069421 5784}{174538289990517578125}\beta^{22}$$
$$- \tfrac{32254495435296445139757114}{45931128944873046875}\beta^{23} - \tfrac{43715635286204172906 375312}{67130111534814453125}\beta^{24} + \tfrac{546580409405561136704024484}{174538289990517578125}\beta^{25} + \tfrac{24953789333492613137822 23032}{872691449952587890625}\beta^{26}$$
$$- \tfrac{68222010936777742973 2601484621372}{48718000193603218994140625}\beta^{27} - \tfrac{728104326241248730928651925895608}{5771209253703765942 3828125}\beta^{28} + \tfrac{5628099088534689327575941379823 53385288}{89543197175840780479040 52734375}\beta^{29}$$
$$+ \tfrac{85199855652798758084022241465749690 10656}{15222343519892932681436889648443 75}\beta^{30} + O(\beta^{31}),$$
$$\text{(F1b)}$$

$$M_G^2 = \frac{4}{3}\beta^{-1} - 4 + \frac{52}{15}\beta - \frac{316}{175}\beta^3 + \frac{5472}{875}\beta^5 - \frac{64}{25}\beta^6 - \frac{19122724}{1010625}\beta^7 + \frac{47808}{4375}\beta^8 + \frac{1316732616}{21896875}\beta^9 - \frac{7823616}{153125}\beta^{10} - \frac{472105313248}{2299171875}\beta^{11}$$

$$+ \frac{1973349088}{8421875}\beta^{12} + \frac{46661184606992}{65143203125}\beta^{13} - \frac{26076544910176}{26823671875}\beta^{14} - \frac{1783696991213198452}{667131543203125}\beta^{15} + \frac{3724145632458848}{938828515625}\beta^{16} + \frac{5630519133419621984}{526682797265625}\beta^{17}$$

$$- \frac{14678226956585492416}{877804662109375}\beta^{18} - \frac{2330772245562856513080 7096}{523614869971552734375}\beta^{19} + \frac{131635204541138381824}{1796123385546875}\beta^{20} + \frac{149312139205839228573 76688}{79335586359326171875}\beta^{21}$$

$$- \frac{12490315953001109355570208}{37943106519677734375}\beta^{22} - \frac{268173518152038112779584900384}{335986208231746337890625}\beta^{23} + \frac{13036400790187358943446 20352}{87269144995258789062 5}\beta^{24}$$

$$+ \frac{3804374894243327260181091787 0624}{112426154292930505371093 75}\beta^{25} - \frac{3516345285680715101509495 3488864}{517418760676889360351562 5}\beta^{26} - \frac{32741212467941707889297214938863984773664}{228335152798393990022155334472656 25}\beta^{27}$$

$$+ \frac{1538444172762671916055304195595 321312}{498015557151506009338378906 25}\beta^{28} + O(\beta^{29}), \tag{F1c}$$

$$M_v^2 = \frac{2}{9}\beta^{-2} - \frac{38}{45} + \frac{1418}{1575}\beta^2 + \frac{2804}{7875}\beta^4 - \frac{4877702}{3031875}\beta^6 + \frac{83484008}{21896875}\beta^8 - \frac{510322072076}{34487578125}\beta^{10} + \frac{241521726513358}{4104021796875}\beta^{12} - \frac{35557059082336258372}{1501045972207031 25}\beta^{14}$$

$$+ \frac{36567597421005478608 23}{3752614930517578125}\beta^{16} + O(\beta^{18}), \tag{F1d}$$

$$M_h^2 = \frac{4}{3}\beta^{-1} - 4 + \frac{52}{15}\beta - \frac{316}{175}\beta^3 + \frac{15296}{2625}\beta^5 - \frac{64}{125}\beta^6 - \frac{6651852}{336875}\beta^7 + \frac{1088}{4375}\beta^8 + \frac{4502031416}{65690625}\beta^9 - \frac{203936}{459375}\beta^{10} - \frac{192671527632}{766390625}\beta^{11} + \frac{1013665088}{294765625}\beta^{12}$$

$$+ \frac{1306699165544048}{1368007265625}\beta^{13} - \frac{1577414046048}{134118359375}\beta^{14} - \frac{187249702135322630044}{50034865740234375}\beta^{15} + \frac{27983550800928}{670591796875}\beta^{16} + \frac{19740602610220039971 2}{13167069931640625}\beta^{17}$$

$$- \frac{561057571773872512}{4389023310546875}\beta^{18} - \frac{94202359765476620058833 68}{15400437352104492187 5}\beta^{19} + \frac{1718319942794918026649 6}{43780507522705078125}\beta^{20} + \frac{33146319869019734063983 91696}{130903717492888183593 75}\beta^{21}$$

$$- \frac{16885280414917672776095 04}{13280087281887207031 25}\beta^{22} - \frac{53446974337526905393761 57188912}{50397931234761950683593 75}\beta^{23} + \frac{71000248992338414512370 9548576}{17639275932166682739257 8125}\beta^{24} + O(\beta^{25}), \tag{F1e}$$

$$u = 3\beta - 27\beta^2 + \frac{1176}{5}\beta^3 - \frac{10233}{5}\beta^4 + \frac{623418}{35}\beta^5 - \frac{27129006}{175}\beta^6 + \frac{9444396}{7}\beta^7 - \frac{82196703}{7}\beta^8 + \frac{983643153048}{9625}\beta^9 - \frac{299630551162554}{336875}\beta^{10}$$

$$+ \frac{169503983781937692}{21896875}\beta^{11} - \frac{1475232154782748902}{21896875}\beta^{12} + \frac{987637288715664984}{1684375}\beta^{13} - \frac{50792385588434618148}{9953125}\beta^{14} + \frac{82664811252077369258388}{1861234375}\beta^{15}$$

$$- \frac{3525309240917592383822 0943}{91200484375}\beta^{16} + \frac{15694806775998694225868 699994}{4665255546875}\beta^{17} - \frac{19931794277023069367006 32573158}{68074647265625}\beta^{18}$$

$$+ \frac{17000157016977567976729 7711329632}{667131543203125}\beta^{19} - \frac{73978138304534583264080 00754198846}{3335657716015625}\beta^{20} + \frac{74042606580284578369030 51615667215212}{383600637341796875}\beta^{21}$$

$$- \frac{11728258998889165869855 099963759764004972}{6981531599620703125}\beta^{22} + \frac{12759216950536912218962 9344484949460211245084}{87269144995258789062 5}\beta^{23}$$

$$- \frac{15863771397300216952075 97176428886904094 38}{124670207136083984375}\beta^{24} + \frac{96646235832092490263933 0987486375983311624744}{87269144995258789062 5}\beta^{25}$$

$$- \frac{22135116299712607238671 1604146938113185602308}{229655644724365234375}\beta^{26} + \frac{40867173106509863686061 77681425627716599608131 58664}{48718000193603218994140 625}\beta^{27}$$

$$- \frac{27387083348707117480742 0156540338331788208519 364045012}{37512860149074478625488 28125}\beta^{28} + \frac{56895597608918353629354 633614576615665036036136 28700393824}{89543197175840780479040 52734375}\beta^{29}$$

$$- \frac{42089915133537648667162 70905427277208225624532 61794820086 5512}{76111717599466634071844 482421}\beta^{30} + O(\beta^{31}). \tag{F1f}$$

2. N=4

$$E = \beta - \frac{2}{3}\beta^3 + \frac{8}{3}\beta^5 - \frac{512}{45}\beta^7 + \frac{6254}{135}\beta^9 - \frac{112352}{567}\beta^{11} + \frac{495496}{567}\beta^{13} - \frac{501611216}{127575}\beta^{15} + \frac{11453817058}{637875}\beta^{17} - \frac{748041961864}{9021375}\beta^{19} + \frac{4879081930372}{12629925}\beta^{21}$$

$$- \frac{468805978966751344}{258597714375}\beta^{23} + \frac{5164375543360356758}{603394666875}\beta^{25} - \frac{3308377214206458689408}{81458280028125}\beta^{27} + \frac{5256059401974658161694}{27152760009375}\beta^{29} + O(\beta^{31}), \tag{F2a}$$

$$\chi = 1 + 3\beta + 6\beta^2 + 10\beta^3 + 16\beta^4 + 26\beta^5 + \frac{110}{3}\beta^6 + \frac{598}{15}\beta^7 + \frac{752}{15}\beta^8 + \frac{4492}{45}\beta^9 + \frac{1114}{9}\beta^{10} - \frac{21976}{945}\beta^{11} - \frac{18344}{315}\beta^{12} + \frac{622724}{945}\beta^{13}$$

$$+ \frac{11892428}{14175}\beta^{14} - \frac{102416012}{42525}\beta^{15} - \frac{19192244}{6075}\beta^{16} + \frac{10289936}{875}\beta^{17} + \frac{9473001266}{637875}\beta^{18} - \frac{1147872224624}{21049875}\beta^{19} - \frac{285404814608}{4209975}\beta^{20} + \frac{5401807541912}{21049875}\beta^{21}$$

$$+ \frac{138663144738428}{442047375}\beta^{22} - \frac{14938117796303512}{12314176875}\beta^{23} - \frac{1260279869167333444}{86199238125}\beta^{24} + \frac{386190762389548268}{67043851875}\beta^{25} + \frac{1379265161509279622}{201131555625}\beta^{26}$$

$$- \frac{745692645593229011368}{27152760009375}\beta^{27} - \frac{878237978318189566412}{27152760009375}\beta^{28} + \frac{356775453663918490943 6}{27152760009375}\beta^{29} + \frac{178390269549069274163 8}{11636897146875}\beta^{30} + O(\beta^{31}), \tag{F2b}$$

$$M_G^2 = \frac{4}{3}\beta^{-1} - 4 + \frac{32}{9}\beta - \frac{56}{27}\beta^3 + \frac{2944}{405}\beta^5 - \frac{8}{3}\beta^6 - \frac{30136}{1215}\beta^7 + \frac{376}{27}\beta^8 + \frac{2169952}{25515}\beta^9 - \frac{27872}{405}\beta^{10} - \frac{17364176}{54675}\beta^{11} + \frac{139568}{405}\beta^{12} + \frac{1403817608}{1148175}\beta^{13}$$

$$- \frac{206305088}{127575}\beta^{14} - \frac{12041211784}{2460375}\beta^{15} + \frac{44783968}{6075}\beta^{16} + \frac{2327367655528}{113669325}\beta^{17} - \frac{5538622408}{164025}\beta^{18} - \frac{1056805727795792}{11935279125}\beta^{19} + \frac{2704092978728}{17222625}\beta^{20}$$

$$+ \frac{909455600757890632}{2327379429375}\beta^{21} - \frac{4903884524065528}{6630710625}\beta^{22} - \frac{85272481476107112904}{48874968016875}\beta^{23} + \frac{19055775959948008}{5425128675}\beta^{24} + \frac{82183692719025324516 8}{104732074321875}\beta^{25}$$

$$- \frac{7802995733962068568}{465475885875}\beta^{26} - \frac{15607345431297974660104}{439874712151875}\beta^{27} + \frac{19608530438150678273776}{244374840084375}\beta^{28} + O(\beta^{29}), \tag{F2c}$$

$$M_v^2 = \frac{2}{9}\beta^{-2} - \frac{22}{27} + \frac{8}{9}\beta^2 + \frac{494}{1215}\beta^4 - \frac{8284}{3645}\beta^6 + \frac{161257}{25515}\beta^8 - \frac{3197867}{127575}\beta^{10} + \frac{40478257}{382725}\beta^{12} - \frac{23351747878}{51667875}\beta^{14} + \frac{2016622630922}{1023023925}\beta^{16} + O(\beta^{18}), \tag{F2d}$$

$$M_h^2 = \frac{4}{3}\beta^{-1} - 4 + \frac{32}{9}\beta - \frac{56}{27}\beta^3 + \frac{2764}{405}\beta^5 - \frac{16}{27}\beta^6 - \frac{30376}{1215}\beta^7 + \frac{64}{81}\beta^8 + \frac{2357776}{25515}\beta^9 - \frac{184}{135}\beta^{10} - \frac{19782236}{54675}\beta^{11} + \frac{76984}{10935}\beta^{12} + \frac{1686885896}{1148175}\beta^{13}$$

$$- \frac{2132936}{76545}\beta^{14} - \frac{5039762128}{820125}\beta^{15} + \frac{76496944}{688905}\beta^{16} + \frac{2987093529676}{113669325}\beta^{17} - \frac{22231013972}{51667875}\beta^{18} - \frac{50559997058744}{442047375}\beta^{19} + \frac{775676060228}{465010875}\beta^{20}$$

$$+ \frac{391764598151298668}{775793143125}\beta^{21} - \frac{512747827960696}{76726794375}\beta^{22} - \frac{110242538271813248108}{48874968016875}\beta^{23} + \frac{43888147443715136}{1611262681875}\beta^{24} + O(\beta^{25}), \tag{F2e}$$

$$u = 3\beta - 27\beta^2 + 235\beta^3 - 2043\beta^4 + 17765\beta^5 - 154479\beta^6 + \frac{20149303}{15}\beta^7 - \frac{58403373}{5}\beta^8 + \frac{4570670527}{45}\beta^9 - \frac{13248238489}{15}\beta^{10}$$

$$+ \frac{7257685461779}{945}\beta^{11} - \frac{4207327698821}{63}\beta^{12} + \frac{548777845884239}{945}\beta^{13} - \frac{3408540645268981}{675}\beta^{14} + \frac{1867275863842718053}{42525}\beta^{15} - \frac{51546286924640369}{135}\beta^{16}$$

$$+ \frac{235318541138701614541}{70875}\beta^{17} - \frac{6138706350282887902919}{212625}\beta^{18} + \frac{528459258075001987572771}{21049875}\beta^{19} - \frac{510585477719427773522979}{2338875}\beta^{20}$$

$$+ \frac{3995861481537990978204638 63}{21049875}\beta^{21} - \frac{2432248374621917445334244 1067}{147349125}\beta^{22} + \frac{1237266473669070860765476 68505151}{86199238125}\beta^{23}$$

$$- \frac{717251463309460504958719584 06491}{5746615875}\beta^{24} + \frac{2182925651814838079346684 3521759833}{201131555625}\beta^{25} - \frac{569455321970865221978936 851386596153}{603394666875}\beta^{26}$$

$$+ \frac{2228289567155043434572724885 03713477607}{27152760009375}\beta^{27} - \frac{1318116356461011902773329278 5978467713}{184712653125}\beta^{28} + \frac{168488607495344336394131310 84425510515541}{27152760009375}\beta^{29}$$

$$- \frac{775190057499031799755350461405 515599727}{143665396875}\beta^{30} + O(\beta^{31}). \tag{F2f}$$

3. $N=8$

$$E = \beta - \frac{4}{5}\beta^3 + \frac{46}{15}\beta^5 - \frac{7552}{525}\beta^7 + \frac{2302}{35}\beta^9 - \frac{555317288}{1771875}\beta^{11} + \frac{2746333288}{1771875}\beta^{13} - \frac{1785780786208}{227390625}\beta^{15} + \frac{49727658484666}{1227909375}\beta^{17} - \frac{4222283776631137752}{1995352734375}\beta^{19}$$

$$+ \frac{26014686098048746528}{23279115234375}\beta^{21} - \frac{15104723786912338924452 8}{25383189111328125}\beta^{23} + \frac{10528747447001620271543026}{329981458447265625}\beta^{25} - \frac{5472231864702145478944709 6}{318009342041015625}\beta^{27}$$

$$+ \frac{14125457130390807278617790 2882}{15146148942729492187 5}\beta^{29} + O(\beta^{31}), \tag{F3a}$$

$$\chi = 1 + 3\beta + 6\beta^2 + \frac{48}{5}\beta^3 + \frac{72}{5}\beta^4 + \frac{112}{5}\beta^5 + \frac{746}{25}\beta^6 + \frac{170}{7}\beta^7 + \frac{3392}{175}\beta^8 + \frac{2392}{35}\beta^9 + \frac{1330922}{13125}\beta^{10} - \frac{12052904}{84375}\beta^{11} - \frac{38292976}{118125}\beta^{12}$$

$$+ \frac{509694772}{590625}\beta^{13} + \frac{35255323868}{20671875}\beta^{14} - \frac{201482297164}{45478125}\beta^{15} - \frac{1185431950796}{136434375}\beta^{16} + \frac{33950985399928}{1461796875}\beta^{17} + \frac{2298488652590486}{51162890625}\beta^{18}$$

$$- \frac{409115403009898784}{3325587890625}\beta^{19} - \frac{7816230894808292 48}{3325587890625}\beta^{20} + \frac{2184027254831875996}{3325587890625}\beta^{21} + \frac{18575830815990090084 76}{149651455078125}\beta^{22} - \frac{352812582319144541566 24}{9999438134765625}\beta^{23}$$

$$- \frac{7266174831391645629212 84}{109993819482421875}\beta^{24} + \frac{23958983619315583378 52}{125707222265625}\beta^{25} + \frac{5560379391092949450447 34}{15713402783203125}\beta^{26} - \frac{483516626839965926762147 2288}{46747373280029296875}\beta^{27}$$

$$- \frac{76375110913709387715443574 8}{4006917709716796875}\beta^{28} + \frac{711299012158799734199117996 536}{1262179078560791015625}\beta^{29} + \frac{1002625224890767081865824 27306586}{9718778904918090820312 5}\beta^{30} + O(\beta^{31}), \tag{F3b}$$

$$M_G^2 = \frac{4}{3}\beta^{-1} - 4 + \frac{56}{15}\beta - \frac{608}{225}\beta^3 + \frac{8544}{875}\beta^5 - \frac{56}{25}\beta^6 - \frac{690104}{16875}\beta^7 + \frac{30632}{1875}\beta^8 + \frac{895240544}{5315625}\beta^9 - \frac{2698048}{28125}\beta^{10} - \frac{15337773008}{20671875}\beta^{11} + \frac{78233152}{140625}\beta^{12}$$

$$+ \frac{15033061154264}{4385390625}\beta^{13} - \frac{46357786976}{14765625}\beta^{14} - \frac{1502465010829864}{92093203125}\beta^{15} + \frac{11492930412128}{664453125}\beta^{16} + \frac{1111624153887072856}{13967469140625}\beta^{17} - \frac{3450172284172424}{36544921875}\beta^{18}$$

$$- \frac{3734860553852716409584}{9428041669921875}\beta^{19} + \frac{8295415887259675624}{16116310546875}\beta^{20} + \frac{19826752331731381636250 48}{989944375341796875}\beta^{21} - \frac{3091252475820876533244 56}{109993819482421875}\beta^{22}$$

$$- \frac{16910028827683018859169992}{1649907292236328125}\beta^{23} + \frac{16910969702026167023252 24}{109993819482421875}\beta^{24} + \frac{6684001506578658050398807571 2}{1262179078560791015625}\beta^{25} - \frac{46345645264745356443888008}{549969097412109375}\beta^{26}$$

$$- \frac{120616417598489443051159145115 4792}{43734505072131408691406 25}\beta^{27} + \frac{57262390753050551283591565888}{12374304691772460937 5}\beta^{28} + O(\beta^{29}), \tag{F3c}$$

$$M_v^2 = \frac{2}{9}\beta^{-2} - \frac{34}{45} + \frac{568}{675}\beta^2 + \frac{13784}{23625}\beta^4 - \frac{69604}{16875}\beta^6 + \frac{241041191}{15946875}\beta^8 - \frac{185964672997}{2790703125}\beta^{10} + \frac{1392084587186}{4385390625}\beta^{12} - \frac{10666554935618557}{6906990234375}\beta^{14}$$

$$+ \frac{120272997266688239927}{15713402783203125}\beta^{16} + O(\beta^{18}), \tag{F3d}$$

$$M_h^2 = \frac{4}{3}\beta^{-1} - 4 + \frac{56}{15}\beta - \frac{608}{225}\beta^3 + \frac{24652}{2625}\beta^5 - \frac{224}{375}\beta^6 - \frac{673136}{16875}\beta^7 + \frac{10976}{5625}\beta^8 + \frac{899887928}{5315625}\beta^9 - \frac{480088}{84375}\beta^{10} - \frac{5216665892}{6890625}\beta^{11} + \frac{53139224}{2109375}\beta^{12}$$

$$+ \frac{15464225123456}{4385390625}\beta^{13} - \frac{8888980504}{73828125}\beta^{14} - \frac{38922396533024104}{2302330078125}\beta^{15} + \frac{5789142673744}{9966796875}\beta^{16} + \frac{32467756338289108}{391904296875}\beta^{17} - \frac{36412917799914748}{1279072265625}\beta^{18}$$

$$- \frac{19467809813152568040512}{47140208349609375}\beta^{19} + \frac{85327706507419012316}{6043616455078125}\beta^{20} + \frac{10330548206236154611036876}{4949721876708984375}\beta^{21} - \frac{11713325634025698161 6728}{1649907292236328125}\beta^{22}$$

$$- \frac{8000075417927232351906676}{749957860107421875}\beta^{23} + \frac{16564302174777736394276208}{4583075811767578125}\beta^{24} + O(\beta^{25}), \tag{F3e}$$

$$u = 3\beta - 27\beta^2 + \frac{1173}{5}\beta^3 - \frac{10179}{5}\beta^4 + \frac{88357}{5}\beta^5 - \frac{3834927}{25}\beta^6 + \frac{9320831}{7}\beta^7 - \frac{404542143}{35}\beta^8 + \frac{87789657841}{875}\beta^9 - \frac{3810245382897}{4375}\beta^{10}$$

$$+ \frac{4465049407354747}{590625}\beta^{11} - \frac{4306488725191523}{65625}\beta^{12} + \frac{336438262155902647}{590625}\beta^{13} - \frac{3785726352066159219}{765625}\beta^{14} + \frac{9759896773518266783449}{227390625}\beta^{15}$$

$$- \frac{28239924187021013712337}{75796875}\beta^{16} + \frac{330930542941961427975065 11}{10232578125}\beta^{17} - \frac{161201362792739168226539 3}{57421875}\beta^{18} + \frac{16207996051281750382556862 3029}{665117578125}\beta^{19}$$

$$- \frac{1421129597490899882904193 8103}{6718359375}\beta^{20} + \frac{4274412982994845258282610 30140363}{23279115234375}\beta^{21} - \frac{2524054350891650540874198 6975703}{158361328125}\beta^{22}$$

$$+ \frac{15217993941616253793162166 2918853279261}{109993819482421875}\beta^{23} - \frac{14677579936524706903155075 5820556182991}{12221535498046875}\beta^{24} + \frac{11466649049267256355353232 3832429180274931}{109993819482421875}\beta^{25}$$

$$- \frac{5529725490442019505149533 6139745677825041}{61107677490234375}\beta^{26} + \frac{3672015995832780319237784 83847484819042846311}{46747373280029296875}\beta^{27}$$

$$- \frac{1062485144503393173493863 6334010179827176190 13}{15582457760009765625}\beta^{28} + \frac{5746508983450818802706580 17936704342506323970 31}{97090698350830078125}\beta^{29}$$

$$- \frac{2773992095457174250780490 481514774376937175605656 33}{53993216138433837890625}\beta^{30} + O(\beta^{31}). \tag{F3f}$$

[1] M. Campostrini, A. Pelissetto, P. Rossi, and E. Vicari, in *Lattice 95*, Proceedings of the International Workshop, Melbourne, Australia, edited by T. D. Kieu *et al.* [Nucl. Phys. B (Proc. Suppl.) **47** (1996)], M. Campostrini, A. Cucchieri, T. Mendes, A. Pelissetto, P. Rossi, A. D. Sokal, and E. Vicari, *ibid.*

[2] M. Campostrini, A. Pelissetto, P. Rossi, and E. Vicari, ''A strong-coupling analysis of two-dimensional O(*N*) σ models with $N \leq 2$ on square, triangular and honeycomb lattices,'' Report No. IFUP-TH 6/96 [Phys. Rev. B (to be published)].

[3] H. E. Stanley, Phys. Rev. **176**, 718 (1968).

[4] M. Campostrini, P. Rossi, and E. Vicari, Phys. Rev. D **52**, 386 (1995).

[5] M. Campostrini and P. Rossi, Phys. Lett. B **242**, 81 (1990).

[6] M. Campostrini, A. Pelissetto, P. Rossi, and E. Vicari, Nucl. Phys. **B459**, 207 (1996).

[7] P. Butera, M. Comi, G. Marchesini, and E. Onofri, Nucl. Phys. **B236**, 758 (1989).

[8] I. S. Gradštein and I. M. Ryžik, *Table of Integrals, Series and Products* (Academic Press, Orlando, 1980).

[9] A. J. Guttmann, in *Phase Transitions and Critical Phenomena*, edited by C. Domb and J. Lebowitz (Academic Press, New York, 1989), Vol. 13.

[10] M. Lüscher and P. Weisz, Nucl. Phys. **B300**, 325 (1988).

[11] P. Butera, M. Comi, and G. Marchesini, Phys. Rev. B **41**, 11 494 (1990).

[12] T. Reisz, Nucl. Phys. **B450**, 569 (1995).

[13] P. Butera and M. Comi, Phys. Rev. B **52**, 6185 (1995).

[14] M. Campostrini, P. Rossi, and E. Vicari, Phys. Rev. D **52**, 358 (1995).

[15] P. Rossi and E. Vicari, Phys. Rev. D **49**, 6072 (1994); **50**, 4718(E) (1994).

[16] H. Flyvbjerg, Nucl. Phys. **B348**, 714 (1991).

[17] P. Biscari, M. Campostrini, and P. Rossi, Phys. Lett. B **242**, 225 (1990).

[18] S. Meyer (unpublished).

[19] M. Campostrini and P. Rossi, Int. J. Mod. Phys. A **7**, 3265 (1992).

[20] A. J. Guttmann and G. S. Joyce, J. Phys. A **5**, L81 (1972); D. L. Hunter and G. A. Baker, Jr., Phys. Rev. B **49**, 3808 (1979).

[21] S. Caracciolo, R. Edwards, A. Pelissetto, and A. D. Sokal, Phys. Rev. Lett. **75**, 1891 (1995).

[22] B. Bonnier and M. Hontebeyrie, Phys. Lett. B **226**, 361 (1989).

[23] P. Hasenfratz, M. Maggiore, and F. Niedermayer, Phys. Lett. B **245**, 522 (1990); P. Hasenfratz and F. Niedermayer, *ibid.* **245**, 529 (1990).

[24] U. Wolff, Phys. Lett. B **242**, 335 (1990).

[25] M. Falcioni and A. Treves, Nucl. Phys. **B265**, 671 (1986).

[26] K. Chandrasekharan, *Elliptic Functions*, Grundlehren der Mathematischen Wissenschaften Vol. 281 (Springer-Verlag, Berlin, 1985).

[27] N. I. Akhiezer, *Elements of the Theory of Elliptic Functions*, Translated Mathematical Monographs Vol. 79 (American Mathematical Society, Providence, 1990).

[28] J. Apostolakis, C. F. Baillie, and G. C. Fox, Phys. Rev. D **43**, 2687 (1991).

[29] R. G. Edwards, S. J. Ferreira, J. Goodman, and A. D. Sokal, Nucl. Phys. **B380**, 621 (1991).